

**STUDY THE FLEXURAL BEHAVIOUR OF CONCRETE-FRP HYBRID
BEAMS UNDER THREE-POINT BENDING**

A Thesis Submitted in fulfillment of the Requirement for the Award of the Degree of

MASTER OF ENGINEERING

In Structural Engineering

Submitted by

NEELKANTH CHANDRAMAULI

801724018

Under the supervision of

Dr. Himanshu Chawla

Assistant Professor

Civil Engineering Department



THAPAR INSTITUTE
OF ENGINEERING & TECHNOLOGY
(Deemed to be University)

CIVIL ENGINEERING DEPARTMENT
THAPAR INSTITUTE OF ENGINEERING & TECHNOLOGY
(A DEEMED TO BE UNIVERSITY), PATIALA, PUNJAB
AUGUST 2018

DECLARATION

I Neelkanth Chandramauli hereby declare that the work presented in this thesis entitled “**Study the Flexure Behaviour of Concrete-FRP Hybrid Beams Under Three-Point Bending**” in fulfillment of the requirement for the award of degree of Master of Engineering (Structural Engineering) submitted at Civil Department, Thapar Institute of Engineering and Technology (Deemed to be University), Patiala is an authentic record of work carried out under supervision of **Dr. Himanshu Chawla**, Assistant Professor, Department of Civil Engineering, Thapar Institute of Engineering and Technology, from September 2018 to August 2019. The matter presented in this has not been submitted either in part or full to any other university or institute for the award of any other degree.

Date 11/09/2019

Neelkanth Chandramauli

Neelkanth Chandramauli

801724018

Certificate

This is to certify that the above declaration made by the student concerned is correct according to the best of my knowledge and belief.



Dr. Himanshu Chawla

Assistant Professor

Civil Engineering Department

Thapar Institute of Engineering & Technology

(A deemed to be university), Patiala, Punjab

Date: 10.09.2019

ACKNOWLEDGEMENT

Words are often less to reveals once deep regards for someone. With an understanding that work like this can never be the outcome of a single person, I take this opportunity to express my profound sense of gratitude and respect to all those who helped me through the duration of work. My thesis could not have been completed without the help of many people who contributed directly or indirectly through their constructive criticism. It would not be fair on my part, if I don't say a word of thanks to all those whose sincere suggestions made this period a real educative, enlightening, pleasurable and memorable one.

First of all, a special debt of gratitude is owned to my supervisor Dr. Himanshu Chawla, Assistant Professor, Department of Civil Engineering, Thapar Institute of Engineering and Technology, Patiala for his gracious efforts and keen pursuits, which has remained a valuable asset for the successful completion of my work. His dynamism and diligent enthusiasm has been highly instrumental in keeping my spirit high. His flawless and forthright suggestion blended with an innate intelligent application has crowned my task a success.

I would like to express my gratitude to Dr. Prem Pal Bansal, Head of department of Civil Engineering, Thapar Institute of Engineering and Technology, Patiala for his teaching throughout my Master studies which has given me the required knowledge to complete my thesis.

I would also like to thank my parents and my friends for their constant encouragement & co-operation during the entire period of my thesis work. Last but not least, I would like to thank God for all your good deeds.

Neelkanth Chandramauli

801724018

ABSTRACT

Fiber reinforced polymer (FRP) beams exhibit the brittle failure under three/four-point bending test. Reinforced concrete-FRP hybrid beams show pseudo-ductile characteristics, if the ideal bond formed by mechanical and/or adhesive connectors. Hence, it is important to study the flexural behavior of different connection of reinforced concrete-FRP hybrid beams. In this study, flexural behavior of concrete-FRP hybrid beams is determined. Beams are modeled in finite element software ABAQUS. Shear connection between the FRP beams and RC slab is made using shear connectors and adhesive bonding. Web and flange elements of I-beams are connected with cohesive layer, because it is the weaker portion in the FRP I-beams and is highly prone to fail under three-point loading. Accuracy of the numerical model is verified by comparing the results with published experimental study. Further, the parametric study is performed on beams having different size and spacing of shear connectors. Along with, failure and service load of hybrid beams is determined for different geometric configuration of I-beams and width of RC slab. The flexural response of hybrid FRP-concrete beams obtained from finite element software shows good agreement with experimental testing. It is observed that shear connectors help in improving the strength of concrete-FRP hybrid beams. With increasing the length of shear connectors there is slight improvement in the strength of beam. As density of shear connectors decreases consequently flexural stiffness of the beam (initial slope of load-deflection curve) decreases. It is also noted that strength and stiffness of the hybrid beam increases with increase in the length of the shear connectors. With decrease in the length of the beam, flexural stiffness of the beam increases. The failure and service load is lower for the beams having higher L/d ratio. From the flexural study of the beams having different B/t ratio, it is observed that some beams same failure and service load, it is due to the pre-mature failure of the web-flange junction of the I-beams. Hence, it is stated that addition of RC slab enhances the flexural stiffness, i.e., service load and also enhance the strength of web-flange junction. Addition of reinforced concrete slab over the FRP I-beams, reduces the chances of local buckling of the flange and web of the I-beam.

TABLE OF CONTENTS

	Page No
Declaration	i
Acknowledgement	ii
Abstract	iii
List of tables	v
List of figures	vi
Chapter 1 Introduction	
1.1 Fibres	1
1.2 Fibre reinforced polymer	8
1.3 Shear connectors	12
1.4 Benefit of concrete FRP hybrids	14
1.5 Objectives	14
1.6 Methodology	14
Chapter 2 Literature Review	16
2.1 Composite beam	16
2.2 Connection of FRP concrete hybrid beams	24
2.3 Performance under bending	27
2.4 Numerical modeling of FRP beams	29
2.5 Gaps in present research	30
2.6 Scope and need of present research	30
Chapter 3 Finite Element Modeling	31
3.1 Introduction	31
3.2 Finite element model	32
Chapter 4 Flexural Study of Hybrid Beams	44
4.1 Verification of FE model	44
4.2 Parametric study	45
Chapter 5 Conclusions	52
5.1 Introduction	52
5.2 Conclusions	52
References	53

List of Tables

Table No.	Title	Page No.
3.1	Specifications of various parts	33
3.2	Elastic properties for concrete	35
3.3	Concrete damage plasticity properties for concrete	35
3.4	Compressive behavior properties for concrete	35
3.5	Tensile behavior properties for concrete	35
3.6	Elastic properties of FRP I-Sec beams	36
3.7	Different strength of flange & web elements of FRP I –section	37
3.8	Damage evolution properties for FRP I-section	38
3.9	Plasticity properties of steel bars	38
3.10	Stiffness properties for FRP	40
3.11	Damage evolution properties for FRP	41
3.12	Evolution properties for cohesive element	41

List of figures

Figure No.	Title	Page No.
1.1	Classification of fibres	1
1.2	Abaca fibre	2
1.3	Jute fibre	3
1.4	Rice-straw fibre	3
1.5	Bajra fibre	4
1.6	Cotton fibre	4
1.7	Glass fibre	5
1.8	Carbon fibre	6
1.9	Boron fibre	6
1.10	Aramid-kelvar fibre	7
1.11	Silica-carbide fibre	7
1.12	Pultrusion process	9
1.13	Hand lay-up method	9
1.14	Filament winding process	10
1.15	Resin transfer moulding	11
1.16	Spray up method	12
1.17	Shear connector in composite beam girder	14
3.1	Bearing plates	32
3.2	Compressive stress-strain curve of concrete	34
3.3	Elastic-plastic material with progressive damage	37
3.4	Damage evolution criteria	38
3.5	Hybrid concrete-FRP beam with shear connectors	39
3.6	Connection of stiffeners using fasteners	41
3.7	Description of Boundary conditions	42
3.8	Bearing plate with element type R3D4	43
3.9	Meshing of various parts of model and different type of element used	43
4.1	Concrete-FRP hybrid beams modeled in ABAQUS	44
4.2	Comparison of load-deflection response of hybrid beam obtained from ABAQUS with published results	45
4.3	Stress variation in the concrete layer	45
4.4	Flexural behaviour of FRP-concrete hybrid beam	46
4.5	Flexural response of beams with different size of shear connectors	47
4.6	Flexural response of beams with different spacing of shear connectors	47
4.7	Flexural deformation of beam with l/d ratio 7 and slab width 300mm	48
4.8	Effect of l/d ratio on service and failure load	48
4.9	Flexural deformation of beam with b/t ratio 11 and slab width 300mm	49

4.10	Effect of b/t ratio on service and failure load	50
4.11	Failure of web-flange junction	50
4.12	Effect of d/t ratio on service and failure load	51

CHAPTER 1 Introduction

1.1 Fibers

A fiber is basically a long fine continuous thread or filament type material that may be spun into yarns such as cotton or nylon. These are natural or man-made also known as synthetic substance that are significantly longer than their width. Fibres are appropriate for being processed and polished into a fabric by first spun them into yarns and then woven them to form the fabric.

Fibers are basically categorized in two types as shown in Figure 1.1

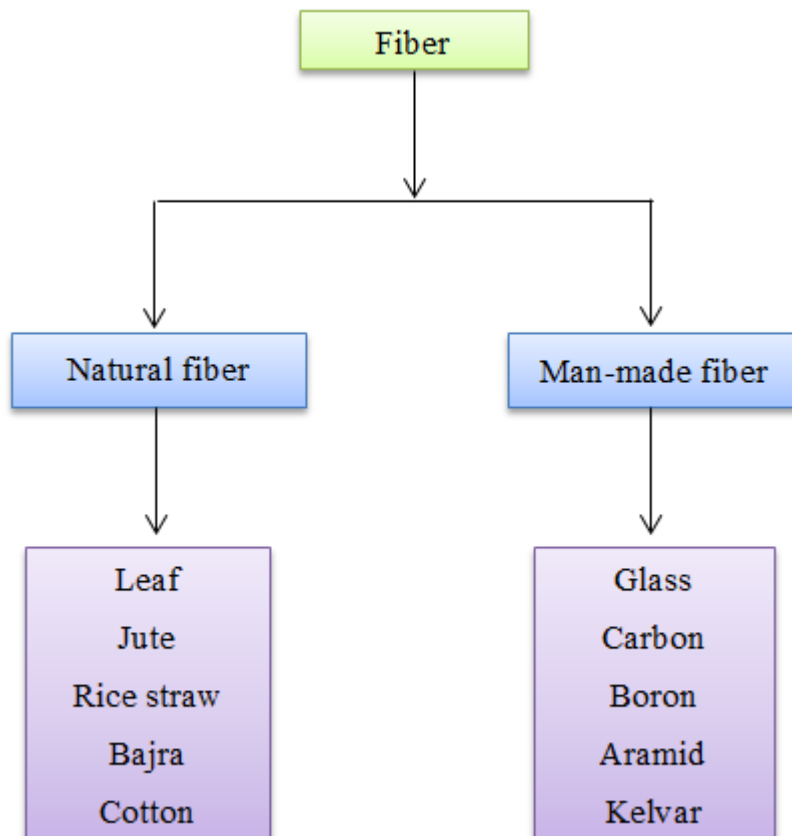


Figure 1.1 Classification of fibers.

(i) Natural fibre

These are defined as those substances which are mainly produced or synthesized from plants and animals, which can be whirl into strand, thread or rope and further be laced, blended, tangled or bounded. A natural fibre can also be broadly defined as an stack or troupe of cells in which the

diameter is minimal in contrast to the length of fibre. Although, the character is flourished by fibrous materials, primarily the plastic sorts like cotton, timber, cereals, and straw, from these solely some are often used in textile industries or for the other industrial functions. Beside from economic purpose of read, the convenience of a fibre for commerce functions square measure determined by properties like length, strength, elasticity, abrasion resistance, absorbency, and varied surface properties. Principally textile fibres square measure slender, flexible, and comparatively robust. They are elastic in nature as they get stretched when put under tension and then partially or completely return to their original length Then tension is removed. The various types of fibers are

(a) Leaf fiber

These are mainly obtained from the sword shaped leaves which are normally thick, fleshy and more often hard surfaced such as agave family plants. These leaves are strengthened and supported through fibre bundles which are very long composing of many cells which are overlapping, bind together by gummy substances. Fibre basically traverses the length of leaf and dense under the surface of leaf. Abaca plant have fibre bundles concentrated in the stalks which is an exception case These leaves are harvested through hand and after that the fibres are separated from the surrounding leaf tissue by machine or hand scrapping or peeling process and after that they are cleaned and dried. Fibre bundles which are not separated into individual fibre cells are known as fibres in trade usually.



Figure 1.2 Abaca fibre.

(b) Jute fibre

These fibres are basically soft, long and shiny in nature which can be spun into coarse type strong threads. These are primarily produced from plants of the genus corwas origin. Corchorus, olitorious are the primary source of the fibre. Jutes are basically the name given to plants and fibres that is used to make gunny cloth. These fibres are used in the manufacturing of rope, wire and aeroplane panels by the use of sugar.



Figure 1.3 Jute fibre.

(c) Rice straw

While harvesting paddy, Rice straws are mainly the by- product produced. These area unit separated from the grains when the plants area unit threshed either manually, or victimization stationary threshers. These are unit comprised of in the main 3 elements polysaccharide, hemicelluloses and polymer that may well be fractionated through pre-treatment. Lignin is a cell wall whereas celluloses are fibre organics. The high content of potassium, ash, alkali leads to agglomeration, fouling and melting in the components of boilers. The uncompressed rice straw have a specific weight about 65-80 kg/m³ with moisture content close to 15-20%. The content of volatile matter in rice straws are higher to those in wood and coal. The large content of ashes in rice husk hampers the energy conversion process. But due to high silica content they wear out during the processing machines like conveyers and grinders and hampers the digestibility for livestock.



Figure 1.4 Rice straw fibre.

(d) Bajra fibre

These are commonly known as pearl millet. These fibres are rich in compounds like iron, magnesium, phosphorous and protein. It consists of important amino acids and vitamins that contributed to its therapeutic properties. They help in weight loss, and are powerful in controlling diabetes and also helpful in digestion as bajra is rich in insoluble fibre that aid in digestion. It reduces secretion of bile acids and it also leads to a lowered risk of gallstone formation. It also

stabilizes the level of cholesterol in the body.



Figure 1.5 Bajra fiber.

(e) Cotton fibre

Cotton is basically a soft fibre that grows around the seeds of the cotton plant. Their growth is in the boll of cotton plant and the seed pod. Each fibre is a single elongated cell that is same as ribbon type with a wide inner hollow and flat twisted. Their building blocks are basically cellulose which forms only when temperature is above 21 degree C. The length of the fibre is the main determining factor of the quality of fibre. Cotton has a natural affinity for water and it aids to evaporation and cooling as moisture passes freely through cotton. Its fibre length ranges from .5 to 2 inches and has a poor resistance against shrinkage and wrinkle with poor acid resistance less abrasion and prone to damage by mildew and moths. It regains moisture around 8% and increase in strength when wet around 10%. The arrangement of cellulose provides cotton durability, strength and obsorbency with no pilling problems and resistance to alkali.



Figure 1.6 Cotton fibre.

(ii) Man-made fibre

These are unit fibre whose chemical composition, structure, and properties area unit considerably

changed throughout the producing method. artificial fibre area unit spun and woven into an enormous range of client and industrial product, as well as clothes like shirts, scarves, and hosiery; home furnishings like upholstery, carpets, and drapes; and industrial components like tire wire, flame-proof linings, and drive belts. The chemical compounds from that man- created fibres area unit made also are referred to as polymers, that area unit a category of compounds characterised by long, catenulate molecules of nice size and relative molecular mass. One amongst the options common to any or all the fibre-forming polymers may be a linear structure. The various types of natural fibre are described next:

(a) Glass fibre

These are made up of extremely fine fibres of glass. Fibre glasses are light weight, extremely strong and act as a robust material. Their strength is lower in comparison to carbon fibre and these are less stiff and brittle in nature but less expensive to carbon fibre. These can be manufactured using moulding process and it's weight properties and bulk strength are higher compare to metals. A type glass fibre is closer to window glass in its composition and c type shows better resistance to chemical impact. E type has characteristics of C type with good insulation to electricity and the AE type shows the property of alkali resistant. In general, glass composes of feldspar, potash, quartz sand, soda with refining and dyeing additives. They have high ratio of surface area to weight but more surface area makes them more susceptible to attacks by chemicals



Figure 1.7 Glass fibre.

(b) Carbon fibre

Carbon fibres are basically a polymer and are also known as graphite fibres. They are very strong and light weight material. These are twice as stiff as steel and five times stronger than steel. These are ideal for various manufacturing material as these are lighter than steel. These are made up of crystalline filaments of carbon which are thin and strong in order to strengthen various materials. These fibres get their strength when twisted together with yarn and it can be thinner than a strand of human hair. They can be woven together in order to take a permanent shape and to form cloths.

They can be laid over a mould thus coated in resins or plastic according to use. These are used in the manufacturing of aircraft wings, tubing, propeller, container and many more according to the situation. These are classified according to the modulus of fibres.

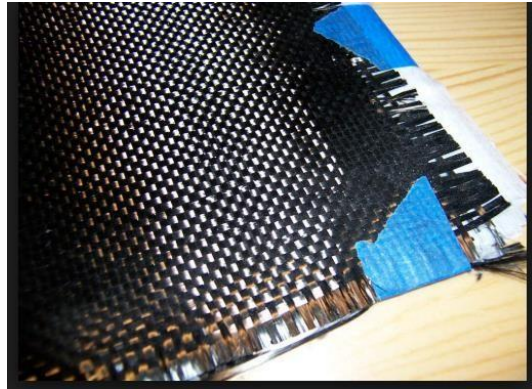


Figure 1.8 Carbon fabric.

(c) Boron fibre

These fibres are produced by CVD, i.e., chemical vapour deposition in a single filament reactor. These fibres comprised a unique combination of high strength and modulus and large diameters in an amorphous element boron product which shows the vast industrial use of free boron. They are commonly used in the construction of high tensile strength tapes. They are used for advance aerospace structures as a component of composite material and also used for golf clubs and fishing rods. The density fibre depends on the substrate and fibre diameter and is sometimes within the vary of 2.3 to 2.6 g/cm³. They rapidly recrystallize at the above 600 degree °. In the reactor a filament is normally supplied through the seals of mercury and filament is heated by direct the effect of direct current.



Figure 1.9 Boron fibre.

(d) Aramid kelvar

These are basically an aromatic polyamide, i.e., characterize by rigid crystalline polymer long chains. Coating, twisting, extrusion, pultrusion and precision winding are the various steps for fibre line enhancing processes for Kelvar. These are used in manufacturing various products such

as rip cords, strength members, industrial fabric yarn and many more. These fibres have normally high strength to the weight ratio, low elongation to break, have good heat and flame resistance, good resistance against chemicals and cut and have marvellous ballistic properties. These fibres have a high melting point above 500°C. A bigger proportion of attractive force contributes to fibre strength as compared to the different fibres.

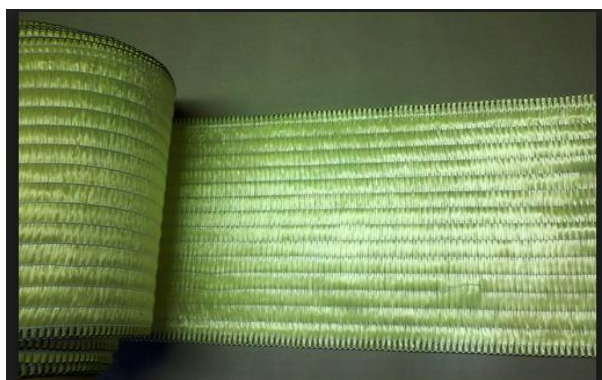


Figure 1.10 Aramid kelvar fibre.

(e) Silica carbide

These fibres provides high resistant against oxidation and are extremely strong thus used for higher temperature applications prevailing in both alpha and beta –Sic compositions. There are two types of silica carbide fibres and two methods for manufacturing of these types of fibres. The first method is a gas phase synthesis on a filament substrate similar to one used for boron fibres. In this the diameter of carbon filament is taken around 30-35 microns. The other method for producing Sic fibres are based on pyrolysis of poly-carbosilance filaments. Thus the resulting fibres consists a mixture of oxygen and carbon in addition with nano size crystalline silicon carbide.

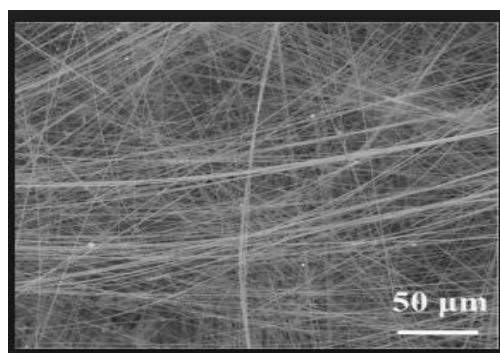


Figure 1.11 Silica carbide fibre.

1.2 Fibre reinforced polymer

Fibre Reinforced Polymer (FRP) is a composite material of a polymer reinforced in fibre. The

composite material consists of a dispersing material that forms a framework of continuous network. These composites are anisotropic as compared to steel and aluminium which are isotropic in nature. It means that the best mechanical properties have orientation in the direction of fibre placement. These materials have mostly have high ratio of strength to density but their brittle nature affects the rate of loading and other environment issues. Fibre reinforcement basically helps to carry the load along the length of fibre and to provide stiffness and strength in one particular direction. The type of fibre controls the nature of composites like carbon, glass and aramid are the three fibres of major types used as reinforcing material and termed as CFRP OR GFRP representing carbon and glass respectively. The matrix helps in transferring forces between the fibres and also protects them from any detrimental effect. Thermosets are basically used as resins and epoxy is preferred over vinyl ester due to creep and chemical resistance but it is also more costly. They help significantly in the safety and economy of the construction works

The various methods used in manufacturing of FRP are:

- i. Pultrusion process
- ii. Hand lay-up method
- iii. Filament winding
- iv. Resin transfer moulding
- v. Spray up method
- vi. Vacuum intrusion
- vii. Reaction injection moulding

(i) Pultrusion process

In this process there is continuous production of composite profile with constant cross section and ideal material properties are made for the required purposes. This process ensures high quality of fibres produced continuously. The process starts with pulling the reinforced material continuously with a guide and placing the fibres according to their profile cross section. After that fibres are impregnated with matrix material in the processing equipment. The mixture of fibre and matrix are pulled through heated equipment in which the curing of profile is done in its final cross section. After this, forward pulling of the most cured profile to a flying saw where the profile is cut into the required length. For good qualities and properties of final products there is a need of proper positioning of fibre and mats in coordination to the profile cross section. The degree of impregnation prevailing in the fibre is a very important factor for the finished good properties.

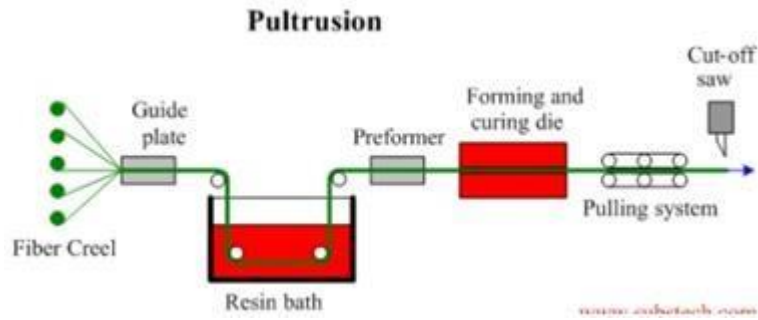


Figure 1.12 Pultrusion process.

(ii) Hand lay-up method

It is a type of moulding process in which the fibre reinforcement are placed by hand and after that they are wetted with resin. It allows for any reinforcing material to be used as raw material due to their manual nature of work and can be easily chopped or mat. The various tools used in this process were typically composite tools which were single sided. The parts in this process have only smooth and visible side. During the *moulding* process a gel code can be added in order to produce cosmetic finished surfaces. This process provides flexibility in the material design with low cost of the tools utilized and this process is suitable for low volume concentrations. But this process has some disadvantages like it has high cycle time and also produces surfaces with one side smooth and moreover inconsistent in the thickness of various parts. In this low density materials like end grain balsa and honeycomb were used in order to stiffen the laminates which are also known as sandwich construction. FRP and paint rollers with squeezes were used to compact the laminate and wetting the reinforcement throughout in order to remove the entrapped air.

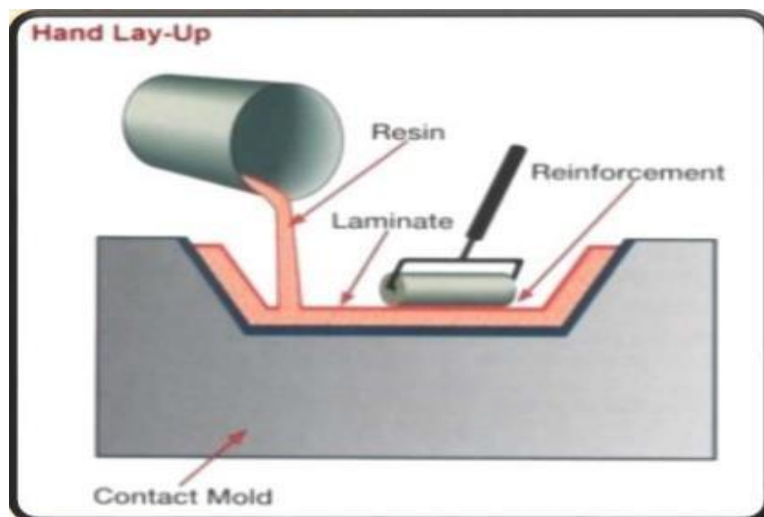


Figure 1.13 Hand lay-up method.

(iii) Filament winding process

This process is basically utilized for oval, circular or hollow sectioned components like tanks or

pipes. In this, tows of fibres are passed through a bath of resin prior to being wound onto a mandrel in various types of orientation which are controlled by the mechanism of fibre feeding and the rotation rate of the mandrel. In this process resins like polyester, epoxy, vinyl ester or phenolic are used and also straight fibres which are not woven or stitch in fabric form. All components are generally single skin type. The main advantage of this process is that it is very fast and thus it leads to economic method in laying of material. The content of resin can be controlled by metering it onto every fibre tow with the help of dies. Due to the absence of any secondary process to convert fibre into fabric before it is used makes the fibre cost minimal. Since there is provision of laying straight fibres into complex pattern in order to match the applied loads ensuring good structural properties of laminates. But the process is only valid for convex shape not concave components. The cost of the mandrel is high and there is problem laying fibre along the component length. This process is used in making pipelines, gas cylinders, chemical storage tank etc.

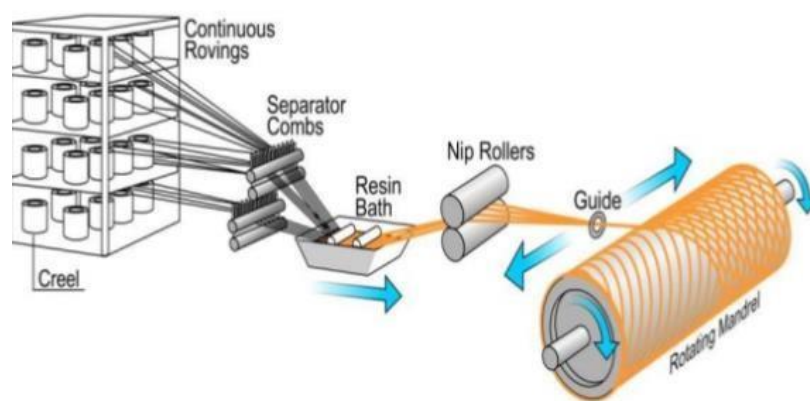


Figure 1.14 Filament winding process.

(iv) Resin transfer moulding

This method produces intermediate composites by volume moulding process. In this method a resin is injected under the influence of pressure into the mould cavity. In this the reinforced materials are laid dry inside the mould. We can adopt a 3d reinforcement or any combination of material according to the use. Tool cavity helps in determining the thickness of the part. In this a gel coat is applied on the mould and the mould is clamped and closed. Resins are injected inside the mould under pressure by injection equipment and the part is cured. Reinforcement can either be a preform type or a pattern cut roll stock material. This method can be performed at the room temperature but higher cycle times can be achieved by the heated moulds. Polyester or epoxy moulds can be used as soft tools while electroformed nickel shell or machine steel moulds can be utilized as a hard tool. In this clamping can be achieved either by press clamping or perimeter clamping. This process can take benefit of broad range of tools of any process required for

composites.

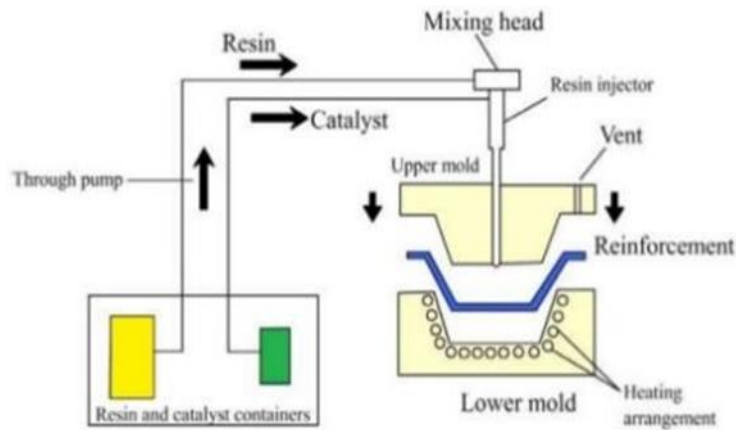


Figure 1.15. Resin transfer moulding

(v) Spray up method

In this process fibre is chopped in gun held in hand and then it is put into a spray of catalyzed resin at the mould position. The material required in this process are resins primarily polyester and fibres having glass roving only. But in this process the cores are to be incorporated separately. This process is advantageous as it provides economical way of depositing fibre and resin quickly. The tools used are also very economical. But the laminates are very resin rich and thus it becomes very heavy. Only small fibres are included which limits the mechanical properties of laminate. The resins have high styrene content which tends to be harmful and they have a tendency to penetrate clothing due to their lower viscosity. This process is mainly utilized in the production of structural panels which are lightly loaded, i.e., truck fairings, bathtub shower trays and many more. There is difficulty in limiting the airborne styrene concentrations to legislative levels. Moreover chopped laminates have better conformability and its production rate is faster as compared to hand lay-up method.

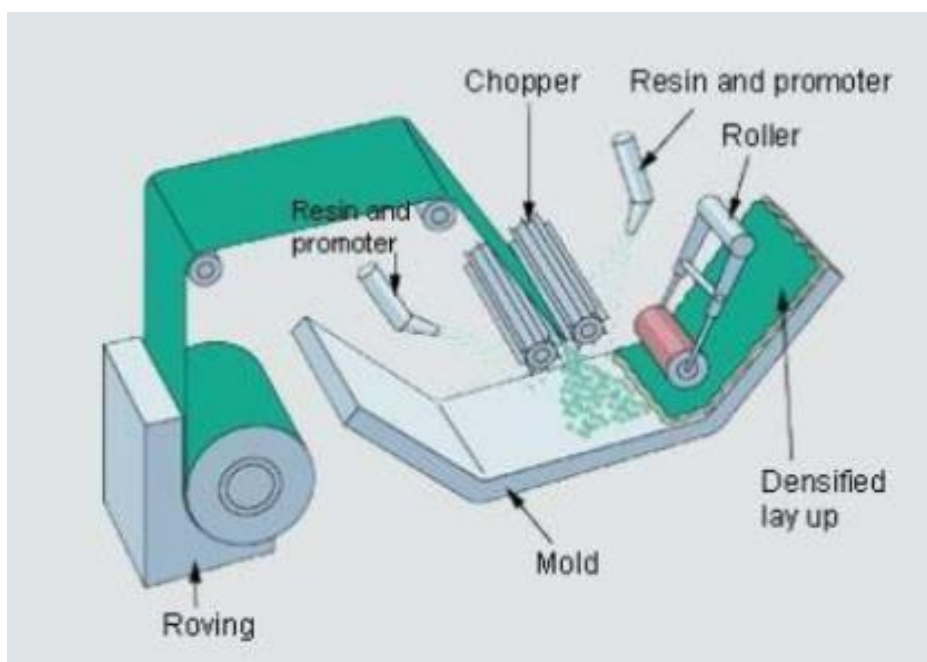


Figure 1.16. Spray up method

1.3 Shear connectors

Shear connectors are basically provided at the portion of top flange of steel concrete or FRP bridge girder of composite action in order to transfer the shear between the slab of composite section and the steel girder so both the structures can perform monolithic action.

The shear connectors are of various types such as

- (i) Headed stud
- (ii) Block and hoop connectors
- (iii) Channel connectors

Block, hoop or channel connectors are provided mostly required in circumstances where large transfer of shear is required. These can be used in place of headed type of shear connectors for closely spacing condition. They strengthen the structural performance by improving strength of material under static or permanent load and the loading due to fatigue action.

In shear connectors shear flows are computed at the quarter, mid-span and at the support- sections so that to make the diagram of flow of shear along the girder. These connectors resist shear at their pivotal positions. Thus the spacing of shear studs can be varied as we move from support to mid span according to our requirement and making the overall structures economical.

In general, the shear studs are available in standard size to be used in the composite structures of height varying from 125 to 250mm at a spacing of 25mm uniformly. The standard diameters of

shear studs generally available are 16, 19, 22 and 25mm. By using a welding gun these shear connectors are attached to the girders flange at top and an arc is provided to connect between the plates of flange portion and the shear connectors. The welding arc connecting the two portions melts them in a fixed amount of time.

The various advantages of using shear connectors or studs are:

- The construction and installation of shear connectors with their welding requires comparatively less time.
- It does not provides a major obstruction or do not hamper the reinforcement of the slabs.
- It helps the concrete to distribute uniformly and the compaction of concrete takes properly around the shear connector.
- It distributes the strength uniformly in all direction.

Some specifications regarding the use of shear connectors are:

- The least distance between the corners of plates of flange and the shear stud is 25mm.
- In case the flange plates are subjected to tensile loading, the diameter of studs should be less than 1.5 times the thickness of plates.
- In case of any other loading case the diameter should be less than 2.5 times the thickness of plate.

Shear connectors are tested by basically two methods:

(i) Ring test

Under this, the side of head of the connector is strucked by a hammer of approximately 2kg. The manner in which the studs generates sound indicates the quality of fusion prevailing, if the sound is ringing it indicates better fusion and vice-versa. All the studs are checked in the same manner through the help of welder.

(ii) Bend test

In this method the head of the stud are displaced in the lateral direction approximately 0.25 times its height by a hammer of nearly 6kg. After this there is need to check the weld for crack propagation and the testing should be assigned according to the design.

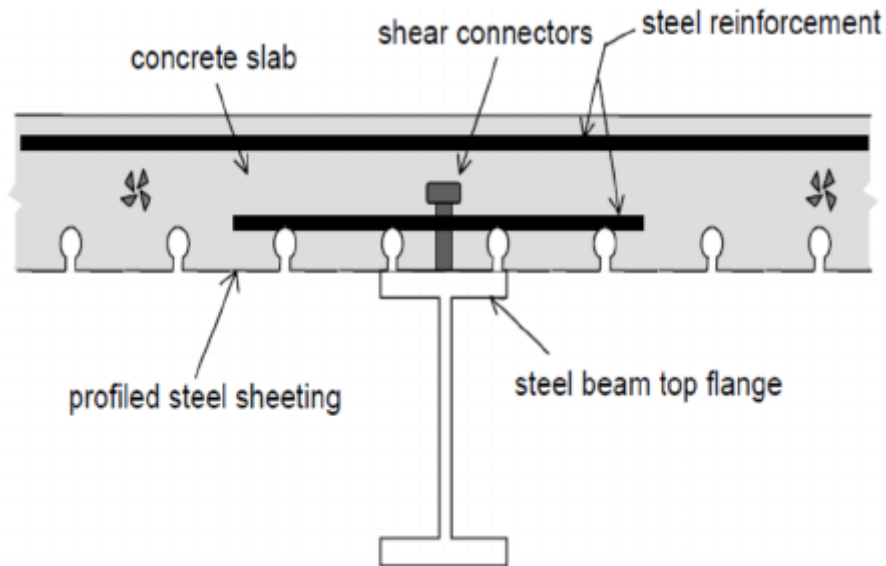


Figure 1.17 Shear connectors in composite beam-girder.

1.4 Benefits of concrete FRP hybrids

It is superior to steel in following terms as it is light weight, corrosion resistant, low expansion rate & many more

1. Steel has weak resistance against fire or high temperature
2. It loses its ductility under certain conditions
3. High expansion rate in changing temperature
4. Heavy material and thus involve expensive transportation
5. Energy intensive to produce

1.5 Objectives

The main objectives of this research work are as follows:

1. Predict the flexural response of FRP-concrete hybrid sections using finite element (FE) software ABAQUS.
2. To determine the effect of length of shear connectors on the flexural behavior of reinforced concrete slab.
3. Evaluate the flexural response of hybrid beams with different sizes of shear connectors.
4. Predict the service and failure loads of the hybrid beam having different geometric configuration of I-beam and reinforced concrete slab.

1.6 Methodology

Based on the objectives set for the present work and the background of research work reported in

literature with the limitations, methodology for executing the proposed result is given as follows:

Phase 1:

Based on the failure modes of FRP beams reported in the literature, FRP beam with reinforced concrete slab is modeled in the ABAQUS considering different failure theories.

Phase 2:

Accuracy of the flexural response obtained from finite element software is checked by verifying the results with published result in literature.

Phase 3:

After the verification of the results, the parametric study is performed on beams having different spacing and sizes of shear connectors.

Phase 4:

Further parametric study is performed on the beams having different length-to-depth ratios, width-to-thickness ratios and depth-to-thickness ratios and different width of reinforced concrete slab.

Phase 5:

The numerical results are analyzed and thesis is written in this phase.

CHAPTER 2 Literature Review

In order to achieve the research objectives listed in Chapter 1, a literature review was conducted on concrete-fibre reinforced polymer hybrid beams. The detailed description of literature review is discussed in the following section

2.1 Composite beam

Hall et al. (1998) analyzed the combined FRP r/f & permanent formwork for concrete members. Replacement of steel re-bars with FRP re-bars or unidirectional GFRP resin composition enhances the mechanical property of structures. They utilized FRP panels & resin burn off test was used to find r/f constraints. They performed two test (1) Bend test & (2) Bond test. In FRP bond test standard 150mm cube mould for concrete was taken. Special loading end plates were made to ensure the resultant vertical loading was applied through neutral axis. In bend test beams were tested 4 point bend according to steel reinforcement. The beam failed under shear & in the FRP panel at web bar interface. Thus we conclude that there should be concrete shear r/f to ensure crushing of concrete as ultimate mode of failure. The reinforcement should be appropriate to optimize the use of materials. Also the voids present in FRP helps the concrete to crack in tension.

Corriea et al. (2007) studied the flexural behaviour of GFRP concrete hybrid beams with interconnection slip. GFRP beams were connected to concrete beams as they have electromagnetic transparency & capability of getting produced in any cross section. A GFRP concrete hybrid beams having appropriate size was taken with their stress-strain distribution curve under four-point bend test. Elastic analysis is performed with full & partial shear interaction. The concrete slab with 100mm height & 400mm wide reinforcement at top & bottom with 15mm cover were used. Load transducer & strain gauge were used to measure loads & displacement. Deformations of concrete GFRP hybrid were due to the summation of deflection due to bending, shear considering the flexibility in the connection. The specimen failed due to bottom flange in tension, web shear failure. Concrete compression failure is the most ductile mechanism leading to a pseudo ductile behaviour with 3 shear test were performed to analyze the behaviour of concrete b/w GFRP & concrete using shear connector system. Material separation also occurred due to failure of bolt due to shear.

Alnahhal et al. (2008) studied the combined behaviour of concrete FRP Bridge on steel beam.

They used hybrid deck system consisting of various units of trapezoidal cell surrounded by outer shell thus leading to the formation of deck of bridge. Concretes were laminated with GFRP model prototype steel bridge of length. Deck model has length & with depth. Bridge decks were comprised of 3 deck panels & each panels had 7 cross sections of trapezoid shape. Shear keys were used & panels were connected for efficient transfer of bending moment & shear force. Gages were placed to measure slip between hybrid deck & girder. There were no traces of cracks or damage in shear connectors thus giving excellent performance of HFRP concrete bridge decks under service loads. But these results are based on parameters used & it can vary rapidly. It also has local moreover, the FRP is designed in tension zone also prior to compression zone which has nothing to do with failure but in return it increases the weight of structure.

Corriea et al. (2009) examined the concrete-GFRP hybrid sections for floors of the buildings. This study provides a novel technique for floors of building with GFRP pultruded profile connected to elements of concrete by adhesive layer of epoxy and steel bolts. Shear connector test was performed on the shear connector in order to examine the flexure behaviour of GFRP beams. Due to geometrical imperfections there is reduction in the flexure behaviour of bonded shear connectors leading to premature failure at low load value. PVC spacers were placed inside the epoxy tar to ensure consistent thickness to adhesive. Results revealed that bonded shear connected system have higher stiffness than bolted connection system. Flexure test was performed & it was concluded that in GFRP I girder lateral bracing helps in preventing the lateral torsional buckling & the failure of the beam was due to the local buckling of the flange at top. Failure of non-strengthened specimen was because of crushing of internet projection section. Thus, GFRP concrete hybrid beams will be used for improvement of the present structures providing higher strength & stiffness.

Correia et al. (2009) analyzed the behaviour of multi span concrete GFRP hybrid beams in flexure. GFRP have high strength, lightweight -weight induction properties. Two shear connection systems between GFRP pultruded & concrete layer was developed one as stainless steel bolts fastened on either side & adhesive layer like epoxy applied on the interface between the two specified materials. Shear connection tests were performed to evaluate strength & stiffness of each shear connection system. GFRP specimen had a fixed cross section & stress strain elastic distribution to analyze the failure. Slab is effective up to the width of concrete & there is full shear interaction between GFRP and slab. Hybrid beams with length 6m were tested in positive & negative bending & load applied at a rate of 0.10m for supports. Failure was due to web shear, web compression & steel bar in tensile & lateral torsional buckling. The lateral

torsional buckling prevents full exploitations of materials strength capacity so lateral bracing must be provided to avoid this.

Gonilha et al. (2010) have studied the creep, dynamic & static behaviour of a full scale GFRP-SFRSCC hybrid footbridge. GFRP pultruded profiles acts as principle support or main girder and SFRSCC slab was set over profile acts as extension bridge deck. An adhesive was provided between the principle support and deck to ensure full collaboration with least slip between the materials. In case of eccentric loading girders were provided to prevent the damage of cross-section. Footbridge prototype was created by first manufacturing & assembling the GFRP main & secondary girders which includes drilling the girder at pre-defined locations to accommodate stainless & anchor. The deck was bonded to stainless steel anchor by using epoxy resin. Footbridge prototype was tested under static load to evaluate vertical deflection & axial strains. The image depicted load deflection curve of linear elastic nature, load-axial strains in both loading & unloading conditions. The creep flexural behaviour was examined under flexural creep test by applying an UDL on top surface of SFRSCC deck. Failure occurred near the web flange junction, initiated at the webs of GFRP main girders. Hybrid footbridge showed adequate structural response by showing the deflection requirement for serviceability limit state. Thus it has been established that GFRP-SFRSCC structural system can be used for footbridges.

Chakraborty et al. (2011) studied the performance of outside filament wound on the hybrid FRP concrete beams. The beam includes CFRP laminates, GFRP pultruded profile & a concrete block wrapped by using filament winding. In order to pin point the lack of degree of stiffness in hybrid beams, CFRP laminates are not allowed to get to failure mode first in order to give indication of forthcoming failure, rather it provides stiffness to beam. The beams were tested under flexure. In the load- displacement curve, beams with steel fibre being reinforced with high strength concrete blocks shows linearity up to failure. The beams having no CFRP reinforcement failed by the lack of native bearing capability of the supports and the other beams failed by crushing of concrete. Thus it is concluded that the dearth of composite action between the concrete block & GFRP box are often solved by wrapping the beams with filament winding.

Kim and Shin (2011) have studied the flexural behaviour of reinforced concrete (RC) beam retro- filled with hybrid fibre reinforced polymer (FRP) under bending test with sustained loading. They performed a four-point bend test on FRP strengthened RC beam and it is compared to the structural behaviour of beam retrofitted by Carbon FRP (CFRP) for in order to enhance the strength in flexure and by Glass FRP (GFRP) for enhancement in shear. CFRP,

GFRP & HFRP sheets are unit materials used below this take a look at with varied loading cases. The beams were reinforced with distorted bars of steel at a good depth and spacing. An adhesive of constant thickness is attached to the FRP layer on the beam. Conjointly electrical gauge connected on beam surface to live concrete strain at middle span. Failure occurred within the type of cracks with vertical cracks and horizontal cracks that propagates into de-bonding of concrete layers, peeling because of shear crack and conjointly delamination of FRP. Thus this test concludes that HFRP improves strength and stiffness of beams by various orientation of their attachment to beams. Also the strengthening effect of HFRP is more in non-preloaded beams than preloaded beams. But the main problem is due to the failure of the retro-fitted RC beam prior to hybrid FRP sheet reach their failure point, thus limiting the strengthening effect of HFRP & leaving a point for further investigation.

Mendes et al. (2011) examined the development of fibre reinforced self-compacting concrete deck and pedestrian bridge having GFRP profile. SCC has high flowing ability while no loss in the stability and is capable of flowing underneath there self-weight fully filled the formwork & accomplishing complete compaction while no vibration. The pedestrian bridge consists of two pultruded GFRP I shape profile connected longitudinally to a SFRSCC. Creep tests were performed on two pedestrian bridge prototypes but the length was half of main span & transverse dimensions were four times smaller than main dimensions. It was observed that the mid surface of SFRSCC deck was under the influence of compressive strain whereas the bottom & top flange of GFRP was under tensile strain. The stresses calculated for both the material was far from their ultimate strength due to deflection concluding that it is necessary to consider creep effect in bridge designs as it is conditioned by limit of serviceability due to deflection.

Dagher et al. (2012) analyzed the bending behaviour of arches made up of concrete with filling of tubular FRP for structures like bridge. For this CFFT were made with nominal diameter & length. The specimen was factory-made with an inward layer of e/g fiber having a texture of fabric at 45degree. The specimen was tested under four-point bend test with hydraulic actuator. Wood saddlers & pads of neoprene were used for supporting of beams. LVDT were used to measure vertical displacement & strain gauge for measuring strains. The abrupt softening occurred under load and is attributed to initial cracking concrete in the tensile zone of span. Failure mode of all specimen were rupture in the tensile region of FRP shell within the two third of the span. In arch test CFFT arches were cast under hydraulic actuator. Failure was rupture of FRP shell in the tensile zone at the location of maximum moment. Further investigations are required to analyze the behaviour of structure & increase design effectiveness

with FRP durability & ductility.

Gonilha et al. (2013) examined the modal identification for GFRP concrete hybrid footbridge prototype. In this, modal identification experimental tests were performed on concrete GFRP hybrid prototype which consists of two GFRP girder of I shape & a SFRSCC deck. In this test an excitation was applied with an impact hammer to the deck & than measuring the applied excitation, response and damping of the structure. Time series of the impact hammer & the corresponding acceleration recorded at the same time at measured points. Frequency range can be determined by using fast Fourier transformation response of the structure.

Nguyen et al. (2015) have analyzed hybrid FRP-UHFPRC composite girders, in which a hybrid FRP I section consisted of CFRP & GFRP laminate as they provide synergistic strengthening effect & long elongation to failure, The UHPFRC provide high degree of ductility & strength in both compression & tension member. Five push out tests were performed at the slab/girder interface to evaluate the shear interaction. The specimen was prepared with & without epoxy resin, in case of epoxy bonded, flange of I section is roughened by sand paper to increase the bond between girder & slab. In the load-slip curve of specimen, slip occurred between girder & slab. This shows that there is slippage of bolt into the region of bearing around the hole in the flange of I girder. Failure modes of specimen were delamination of flange of I girder & severe spalling of slabs indicating that the bolt provided was not efficient to provide the surplus capacity after de-bonding of specimen. Flexural test was also performed to examine the composite behaviour between slab & girder. Failure occurred by crushing of fibres followed by delamination of HFRP girder. In this manner, by the utilization of bolt and epoxy full interaction between slab and girder is obtained and also there is reduction in the stress concentration in the compression flange around the holes.

Neagoe et al. (2015) studied the concrete GFRP hybrid beams with low degree of shear connectors. In this, 8 hybrid beams with GFRP profile were mechanically connected to RC slab. PFRP got inclination over GFRP as later had brittle behaviour under loading. The fabricated beams were exposed to positive moment in 3 point bed test. The specimens in consideration were simply supported with span 1800mm, rested on elastomeric pads. The specimen was loaded with 250kN hydraulic actuator. A pair of elastomer of 200×200×20 mm at support with density 0.75 kg/dc cube was used but it gave conservative results. LVDT & strain gauges were utilized to calculate displacement & strains under loading. The beams failed by yielding of reinforced steel bars at the bottom & by concrete crushing at top. Also cracks due to diagonal

tensile shear were formed near the supports with some lateral torsional buckling. Thus we tend to conclude that GFRP has high ratio of flexural capacity to self-weight magnitude relation value effective. Single GFRP has inferior bending resistance & pseudo ductile behaviour but they have high ultimate capacity. But due to high shear stress concentration there were ruptures of GFRP at web flange section.

Zhang et al. (2015) studied the flexural behaviour of hybrid concrete beam reinforced with Basalt FRP bars. As BFRP have high resistance against temperature, chemical stability, thermal conductivity and corrosion resistance, they prove to be quiet beneficial as a composite material. Pull out test on the specimen is performed until there is destruction thus anchors at the two ends of FRP bars, thus finding the young modulus, tensile strength. A bending test has been done on a hybrid concrete bars r/f with BFRP bars. BFRP bars of 8mm diameter are used as longitudinal reinforcement and standard pull out specimen were utilized to examine the load behaviour between BFRP & concrete with displacement & load detector. The failure happens in 3 ways (1) strains of FRP bar is little however concrete strain is up to final compressive strain that results in over ferroconcrete beam and it leads to brittle failure. (2) strains of FRP bars is larger than design strain and concrete strain is equal to most compressive strain results in brittle failure (3) strain of FRP is a smaller amount than design strain however concrete strain is up to ultimate compressive strain results in ductile failure. BFPC have high bond strength and tensile strength but their large average crack spacing, large deflection and to some extent their elastic modulus is low and there is abrupt in tensile destruction.

Zou et al. (2016) studied the performance of PRFP concrete hybrid beam/deck. Push out test was performed to portray the shear conduct of PFR rib as a method for shear connection of concrete FRP hybrid beam. The specimen included a short segment of FRP I girder connected to small scale concrete slab using shear connector. Fabrications were performed like drilling holes with predefined spacing & diameter and the bolt was set to a predefined embedment length & casting the concrete in timber formwork. The reinforcement bars were product of ribbed steel with yielding strength 235 MPa. The push out test was conducted using a heap of five hundred ton at a stacking rate of 0.5 kN/s. By utilizing typical quality bolts a cracking sound was detected and with increase in load crack also increases and slip happens. FRP cracked along the fibre direction lines between two predrilled holes & shear fracture of perforated FRP plates. Cracking along fibre direction is caused by shear failure. Thus the conclusion drawn is that the ultimate capacity of PFR is 2.5 times greater than the steel bolts & shear resistance ability is 10 times. Also the thickness of plate & space of predrilled holes affect the slip behaviour of PFR according

to slip modulus theory.

Qin et al (2017) studied the impact of reinforcement ratio on the flexural performance of concrete FRP hybrid beam. In order to enhance the strength & flexural ductility of FRP, it has been reinforced with steel bars. The hybrid reinforcement ratio b/w FRP & steel plays a pivotal role on the flexural performance of hybrid FRPRC beams. The impact of reinforcement ratio on the bending performance of concrete beam in both over & under reinforced case using 3d finite element model is examined. The result showed that appropriate hardness, toughness & ductility can be achieved by proper design of reinforcement ratio for hybrid beam. In the load deflection curve there are three ranges namely elastic, cracking & ultimate. The load displacement behaviour of FRPRC beams can be predicted by applying finite element analysis.

Koaik et al. (2017) analyzed the behaviour of concrete GFRP hybrid beams under bending. The FRP used was in pultruded form. Firstly, concrete, GFRP & epoxy adhesive were tested. Six beams of I beam was connected to a pair of blocks of concrete having dimension 100×200×200mm. Two shear connector tests were performed to analyze the behaviour at the interface between GFRP & concrete. Digital image transducers were used to analyze the force slip case. The beams were tested under three-point bend test till failure using an appropriate load with loading rate 4mm/min. In this, we performed the push out test which in case of bolting characterize the interface connection. But in bonding interface the push out test overestimates the ultimate stress at the interface and underestimates the stress in the composite beam during flexure.

Cao et al. (2017) studied the flexural behaviour of expansive concrete beam reinforced with hybrid CFRP enclosure & steel bars. They performed the flexure test on specimen of size 120×180mm & length 1000 mm. They utilized CFRP sheets and fabricated it for linkage with the concrete. Four-point bend test was performed with test machine at a loading speed of 0.03kN/s. Displacement transducers & strain gauges were used to find strains & displacement. Flexural crack appeared at middle of span. CFRP sheet gets continuously ruptured under loading. It also suffers from shear compression failure. The results concluded that that there is de-bonding between CFRP & concrete also CFRP gets premature & there is installation problem and it consumes a lot of energy and results in lag in strains.

Wall et al. (2017) examine the behaviour of bridge deck unit of concrete with FRP. Retrofitting is required in the bridges for longer serviceability & FRP fulfilled that purpose, in general CFRP laminates are used. For this bridge decks units were tested under bending. The specimen was

tested using two hydraulic actuators. The loading in the test was applied at a constant rate until failure. Digital image correlation systems were used for measuring strains on side decks. Deflections were measured using displacement transducers. There was uniform distribution of crack along length between points. It failed due to concrete crushing under the effect of load. Concrete chips were started to get remove from the upper surface of Pc deck unit. The failures were seen in constant moment region. At the bottom CFRP plates were bonded to the deck by adhesives & there were long GFRP beam on soffit of Pc. Thus we conclude that the existing code method provides a conservative method of design for evaluating the capability of hardened Pc deck units of FRP.

Duic et al. (2018) examined the performance of concrete beam with BFRP composite re-bars as reinforcement. For testing, 8 full scaled RC beam specimens being simply supported were tested under four-point bend test. The beams were supported by rollers between plates. The load was measured using 3 load cells, displacement were calculated by 4 LVDT & strain gauges were used for measuring strain. During loading, propagation of flexural cracks occurred in extreme tension fibres of concrete in constant moment region. As load increases shear cracks began to propagate & after cracking there is decrease in stiffness of beam. The beam fails in flexural tension & at low r/f ratio BFRP r/f bars will exhibit greater number of flexural & shear cracking & vice versa. It exhibit low energy absorption capacity with low elastic modulus. Also we should consider the contribution of re-bar in cracking moment for better analysis.

Ashour and Araba (2018) examined the flexural performance of concrete steel/GFRP reinforced hybrid continuous beam. Their analysis is based on hybridization of different type of FRP. Flexure test were carried out for the analysis purpose. In this continuous & simple RC beams were tested of appropriate sizes. It has concrete cover of also. The surface of GFRP is coated by sand in order to improve their bond with concrete & load transfer capacity. Tensile test of GFRP were conducted until failure. Also two prisms were tested for bars to obtain modulus of rupture. There were 4 types of failure modes (1) bar rupture due to GFRP (2) Failure by yielding of steel due to crushing of concrete. (3) shear failure (4) ductile flexural failure. By performing the test we conclude that GFRP does not fail by crushing of concrete but GFRP have low stiffness, high deflection, wider cracks which can be controlled by using steel r/f with GFRP re-bars.

Chellapandian et al. (2019) analyzed the flexural behaviour of RC elements strengthened with HFRP technique. For this, four specimen of square cross section of 230mm with a total length of 2000mm reinforced with 8 bars of 12mm diameter providing a spacing of 100mm c/c. A load

of 2000kN from testing machine was applied at a loading rate of 0.03mm/s under four- point bending test. LVDT was provided in the beam to measure the displaced generated at various point under the load. In the region having constant moment first crack appeared on the bottom side. Beyond peak load there is crushing of concrete. In NSM reinforced beam the mechanism of failure was initiated by multiple cracks formation on the tension region also there is spalling of concrete. We conclude that beams with HFRP shows greater load carrying capacity. They have high energy absorption capacity but there is issue with their ductility which needs to be further investigated.

2.2 Connection of FRP–concrete hybrid beams

Canning et al. (1999) investigated the composite activity of a concrete FRP composite beam. In this, different strategies are analyzed to develop connection so as to give most proficient shear transfer. Unidirectional CF plates bonded to soffit of bar giving quality and weight of plates yet the expense of material is high and it gets precisely harmed. In this flange is located away from the axis of neutral point. The webs are manufactured by constructing a sandwich of face materials made from 45° GFRP & polymer foam core. For shear transfer mechanical bonds using indents, manual layer of adhesive layer like epoxy bonding are applied. Beams are manufactured using vacuum bag with curing at low temperature system of resins & lay-up method. All the beams are tested under 4 point bend test. Loads are applied using hydraulic jack via load cell. LVDT & strain gauges were used to calculate deflection & strains. The shear strength of concrete is 20% of compressive strength shear strength of epoxy resin. The increase in GFRP layers increases flexural rigidity. For efficient shear transfer the best method is by bonding of concrete into shuttering of permanent nature using epoxy adhesives. Direct method bonding gives better control but gives appropriate flexural rigidity & bond remains compact up to failure point.

Joo et al. (2008) investigated on the structural behaviour of shear connector used in FRP & concrete bridge deck system. Shear instrumentality resist the shear force iatrogenic by bending moment due external hundreds. FRP module & shear instrumentality were factory-made by pultrusion method & by hand lay-up method. thrust out take a look at was performed on four specimens coated with sand & to analyze the shear stud. It's composed of FRP module, shear instrumentality at either side of FRP module concrete blocks. The varied parameters were height of FRP shear instrumentality, bonding space b/w FRP module & shear instrumentality of shear transfer. The cylindrical specimen was used with concrete slump of thirteen.5cm combination

size of 25mm. The load was provided on the specimen. Slip & displacement were measured victimization of LVDT. The failures were bonding failure b/w shear connector & FRP module, peeling failure & also the web failure. At the time of loading, the failure due to specimen inclination results in pre-mature failure. Thus the unbalanced failure due to inclination of specimen during loading resulted in pre-mature failure. The specimen with large bond area & higher the height of shear connector can resist higher loads.

Mendes et al. (2009) examined the development of fibre reinforced self-compacting concrete deck and pedestrian bridge with GFRP profile. SCC has high flowing ability while no loss in the stability and is capable of flowing underneath there self-weight fully filled the formwork & accomplishing complete compaction while no vibration. The pedestrian bridge consists of two pultruded GFRP I-shape profile connected longitudinally to a SFRSCC. Creep tests were performed on two pedestrian bridge prototypes but the length was half of main span & transverse dimensions were four times smaller than main dimensions. It was observed that the mid surface of SFRSCC deck was under the influence of compressive strain whereas the bottom & top flange of GFRP was under tensile strain. The stresses calculated for both the material was far from their ultimate strength due to deflection concluding that it is necessary to consider creep effect in bridge designs as it is conditioned by limit of serviceability due to deflection.

Cho et al. (2010) analyzed the performance analysis of concrete FRP composite deck and the shear connection system. In this, shear association system were coated with coarse sand & concrete wedge. It gave excellent composition within the direction of shear however weakened against normal slip however concrete wedge seemed to be effective. Push out tests were performed to analyze the shear behaviour by varying diameter of hole of solid concrete wedge while having no sand covering. FRP modules were bonded using epoxy on the specimen. With the help of displacement control loads were applied at a loading rate with two installed displacement sensors to calculate the slip formation between FRP module and concrete. By increasing the load there is failure of concrete wedge block inside the FRP which leads to growing of slip. The strength of failure increases in direct proportion to the area of the holes drilled. Also conclusion can be drawn that concrete wedge specimen shows reduced sectional rigidity as compared to coarse sand. In order to prevent the normal split and to enhance the performance of bridge deck concrete wedge can be adopted. Also concrete wedge helps in improving the performance of coarse and coating in fatigue.

Correia et al. (2014) examined the concrete-GFRP hybrid sections for floors of the buildings.

This study provides a novel technique for floors of building with GFRP pultruded profile connected to elements of concrete by adhesive layer of epoxy and steel bolts. Shear connector test was performed on the shear connector in order to examine the flexure behaviour of GFRP beams. Due to geometrical imperfections there is reduction in the flexure behaviour of bonded shear connectors leading to premature failure at low load value. PVC spacers were put inside the epoxy tar to ensure consistent thickness to adhesive. Results revealed that bonded shear connected system have higher stiffness than bolted connection system. Flexure test was performed & it was concluded that in GFRP I-girder lateral bracing helps in preventing the lateral torsional buckling & the failure of the beam was due to the local buckling of the flange at top. Failure of non-strengthened specimen was because of crushing of internet projection section. Thus, GFRP concrete hybrid beams will be used for improvement of the present structures providing higher strength & stiffness.

Nguyen et al. (2015) examined shear connections between UHPRFC slabs & FRP beam through the push out tests. In this, effects of bolted shear connectors of inclined/straight nature & effective ratios of depth-to diameter of bolt were investigated. In total 14 push out tests were performed to calculate the load slip behaviour and resistance of bolt shear connectors. The inclined shear connective showed a surplus ductile behaviour than straight bolt shear connective. Below FRP beam connected to UHPRFC block victimization epoxy & bolt shear connectors is shown. Epoxy bonded specimen behaved linearly up to failure & without epoxy behaved non-linearly up to failure load. The failure was due to bearing failure of HRFP flanges, shearing failure of steel bolts on UHPRFC slab. Also steel bolt shear connectors have higher ultimate resistance in UHPRFC slab than as compared to manufactured once.

Zou et al. (2016) studied the shear key connection and stay in form by concrete FRP hybrid beams/decks. The performance of FRP stay in place (SIP) form, FRP shear key connector & their combination for concrete FRP hybrid beams were calculated under shear with specimens under four-point bend test. There were fabrications by drilling holes in FRP, preparing surface of FRP girder, casting concrete in form work. The failure occurred in a pure shear mode when the bolt shank under the effect of push out test. Also failure is at FRP flange in a shear mode out. There is de-bonding between SIP & FRP. Thus it indicates that the connector system of concrete FRP hybrid beams consists of I girder & concrete slab. SIP ensures full composite action by providing substantial initial bond strength. For efficient use of shear key slip must be provide in an appropriate manner.

2.3 Performance under bending

Saiidi et al. (1994) analyzed the bond behaviour of graphite/epoxy concrete composite beams. The materials used were graphite/epoxy section & concrete slab. It should be remembered that glass/epoxy (By using filament winding plates were manufactured consisting of 42 layers in symmetry method & bond b/w concrete & plate provided by adhesives like epoxy resin with the pot life of 30 min at 25°C. The concrete have maximum aggregate size of 10mm. Sensitivity b/w between bonding is to be analyzed. Compression load was applied on the top of plate with dial gauge measuring displacement. In load deflection curve up to peak point no slippage after that slippage begins. In bend test beams were loaded to failure to determine flexural & shear behaviour of g/e section & concrete sides. Laminates were selected in constructing beams with ply. After the beam failed in web when a vertical crack is formed in short span at the edge of loading plate. Failure also occurred when a de-bonded part of flange of G/E beam buckled & also shear failure as crack propagates. Thus using G/E section with concrete in bridges is an effective method but few constraints like proper optimization of fibre orientation, the cost factor and lack of effective bonding methods raises some issues which is needed to be investigated/E) section should be bonded to concrete rather welding in case of steel.

Deskovic et al. (1995) dissected the short behaviour of FRP combined concrete beam. The specimens were put to a 3-point curve test till failure occurs and it is seen that beams lacking shear connectors failed due to fracture occurred in CFRP followed by concrete GFRP interface de-bonding. The concrete in compression has stress-strain curve of parabolic nature with multidirectional GFRP characterize by non-linear consecutive law under uniaxial test. Failures were observed in the web due to shear stress & in the beams due to flexure, under normal stresses. The investigation resulted in cost effective composite members with pseudo-ductile characteristics of GFRP concrete with ideal bond obtained by the collaboration of adhesive & mechanical connectors.

Fam & Rizkella (2002) analyzed the bending behaviour of concrete filled with fibre reinforced polymer of circular tubes. In this, the effect of concrete filled cross sectional configuration as well as tubes with central hole is examined. Beams were checked in bending under four-point bend test. The beam specimen is set up considering range of span of beam. Different kinds of GFRP holes & a steel beams were accustomed to fabricate the tested beams. Laminates structure indicates the thickness & fibre direction of individual layers. Axial compression check were performed on long GFRP section of tube, Dial gauge for measuring slip, strain gauges & LVDT were used. The impact of concrete stuffed, laminates structure of tube & inner longitudinal holes

were analysed. The failure for wound of hollow filament & GFRP tube were analyzed by concrete flexural & tension failure by rupture of concrete. At loading point the lateral ripping and local crushing of tube, failed by tube splitting in the direction of horizontal shear. The parameters were strength of concrete and tube thickness. Concrete filling provides internal support to tubes, prevents load buckling. But higher stiffness results in lower gain of flexural strength also concrete filled PGFRP tube prematurely fails by horizontal shear in horizontal direction.

Mohammed and Masmoudi (2010) studied the bending behaviour of steel & FRP RC crammed with FRP tube bars. As steel is susceptible to corrosion thus FRP is useful. Materials used were concrete, steel reinforcement, FRP bars & tubes. The specimen was created from 2 concrete batches with sufficient strength. Sand coated GFRP bars with content of fibre around seventy three percent in vinyl organic compound were used. Four-point bending test were performed on RCFFT & RC beams with parameters FRP tube thickness and transverse reinforcement. Electrical strain gauges were used. From the actuator load was transferred to the beam through a steel spreader unclosed loop actuator. The flexural failure was the dominant failure for RCFFT bars however diagonal shear failure at shear span & failure due to shear compression was the main for RC beams. The failure mode was gradual and ductile. Thus we conclude that beams confined with FRP tube shows less deflection, high cracking load level, high stiffness but the axial stiffness affects the deflection & ductility of RCFFT bars.

Atari et al. (2012) studied the flexural strengthening of concrete beams using various composites of FRP. For this, flexure test was performed on the beam. Wrap fabrics of GFRP & CFRP (unidirectional) were used as composite materials in the test. Before the bonding initiates fabric material on the concrete beam surface are scraped to get rid of the weakest layer of dry paste of cement at surface and cleansed with air nozzle. With-in the flexure check, merely simply supported beams having an equivalent dimension and reinforcement were used. Two steel bars are used respectively for flexural reinforcement at top and bottom. Transverse Steel consisting of stirrups with applicable spacing were used for shear reinforcement. All the beams are subjected to perennial loading up to failure with hydraulic jack. In order to carry out the test a concentrated load at the mid-span is applied at a constant displacement rate under the effect of displacement control. Two varieties of failure were seen (1) Flexural failure (2) Local failure. Flexural failure includes failure under compression before and once after the yielding of steel, shear failure and rupture of FRP strips. Local failure occurs due to peeling of composites off the concrete beam. There was an increase of 14% in strength by using twin layer of FRP composites.

Also the result shows that FRP composites have good elongation at rupture thus improves ductility. But the main concern is that these results are possible only when there is no premature failure of the composite materials took place.

Fang et al. (2016) studied the flexural behaviour of composite concrete slab r/f with FRP grid face sheets. The materials used were FRP face sheets, square FRP grids as they have long fatigue life with excellent corrosion resistance. Four-point bend test was performed on the specimen having clear span 1200mm. Three LVDT were utilized to calculate displacement and strain gauges were installed to measure strains. The test was performed using testing hydraulic machine. Cracks were observed as the load increases in the concrete in bending region of CFGF slabs. Delamination between FRP grids & face sheets occurred with increase in loading. We observed that concrete crushes in compression zone & FRP face sheet ruptured in tension zone. Also the concrete portion failed in shear. The results were affected by face sheet thickness as it increase the stiffness proportionally & the rib height can be reduced by enhancing the bending stiffness & ultimate bearing capacity of CFGF slabs but the thickness of FRP face sheets depends on shear rigidity's of FRP tubes.

JU et al. (2017) compared the cracking management within the specification of serviceability for concrete FRP beam. In this, ribbed GFRP bar is used as reinforcement in the concrete beam. The bar consists of E optical fibre & vinyl organic compound resin. The parameters influencing cracks width are spacing of crack, the standard of bond b/w concrete & reinforcing bar and also the strains within the bar. The beam was subjected to four-point bend test showing flexural crack pattern. The modes of failures were rupture of GFRP & crushing of concrete. Intended mode of failure was shown by concrete GFRP reinforced beam. The spacing of bar relative to the applied moment was comparatively large for good bond quality compared to inferior bonding. Thus, evaluating the crack serviceability by four specifications has proved quiet effective for cracking control in the beam.

2.4 Numerical modeling of FRP beams

Xin et al. (2017) experimentally & numerically analyzed the in-plane shear & compression performance of pultruded GFRP composite bridge decks as they are adopted for calculating the in-plane shear & compression properties. In this, 2 forms of GFRP webs were used, one single and other uniformly distributed along the span of bridge having web bonded adhesively. LVDT was used to live displacement & strain gauges for activity strains. The specimen was loaded with a continuing rate of loading. Global buckling, cracks at each top & bottom webs because

of de-bonding was the main reason for the specimen failure. Final failure was due to crack in horizontal direction at top & bottom flange bonded adhesively to the webs. The in- plane shear test flange decks were laterally buckled and the specimen failed due to crack at vertical region at top and bottom webs of deck. Thus average web thickened has large effect on the in-plane shear behaviour rather than in-plane compression behaviour. The in-plane shear stiffness calculated by numerical method was closed to experimental results but in case of compression stiffness were 1.7-2.2 times the experimental results.

2.5 Gaps in present research

From the above literature survey, the following gaps have been identified

1. Usage of natural fibres in concrete for ductile failure.
2. Effect of length of shear connectors on the crack behavior of concrete.
3. Providing concrete around the web flange junction to avoid the delamination of beams.
4. Bond behavior of shear connectors.
5. Limited study is available on flexural behavior of hybrid FRP beams, i.e., GFRP-CFRP beams.
6. FRP can be used in fire resistant structures as it does not conduct electricity

2.6 Scope and need of present research

The FRP sections are superior to steel in many aspects as they are more corrosion resistant and is unaffected by moisture. It is also light weight as compared to steel or aluminum section also there flexural strength is stronger with the later. They do not get permanently deform under impact and can be easily fabricated compared to steel. Also there installation cost is smaller as compared to steels. But the one major drawback of FRP is its ductility which is preventing it to be used as a material on a huge scale. So there is a need of proper research in-order to improve the ductility and other aspects so that they can be used uniformly and globally as a construction material.

CHAPTER 3 Finite Element Modelling

3.1. Introduction

In this study, finite element software ABAQUS is used to the hybrid FRP-Concrete I-sections. The ABAQUS software is based on the finite element method and is capable of solving problems related to non-linear analysis of structures apart from linear analysis, and was developed by Karlsson, Hibbitt & Sorenson. The solution given by the software basically involves three stages: ABAQUS pre-processor, ABAQUS solver and the last ABAQUS postprocessor. In the pre-processor stage, an input file is created containing the design for the solver. The solver gives an output file in the visualization. The postprocessor stage is also known as the visual rendering stage, in which deformed shaped is visualized. ABAQUS CAE gives an appropriate and perfect record in the information structure to ABAQUS. In ABAQUS standard, implicit integration scheme is adopted for the FE analysis. In case of explicit, integration scheme is adopted for solving non-linear system and other complex system under the effect of transient loads. The standard configuration apparatus depends on certain calculation which is reasonable for non-direct examination by static technique. The explicit strategy is essentially disposed towards taking care of issues identified with dynamic and depends on express calculation. ABAQUS CAE is similarly conveys both understood and express examination as indicated by the prerequisite of the demonstrating. Any suitable Post processor or ABAQUS CAE can be utilized to give the results of the analysis of the model.

The ABAQUS software creates an environment that projects consistent and simple interface to create, submit, monitor and evaluate the results from the simulations performed in the case of implicit and explicit according to the requirement. ABAQUS CAE is extensively isolated into 2 modules, wherever all of the modules extends and characterizes a legitimate aspect or amount of the demonstrating procedure as an example pure mathematics characterizing, material property characterizing and making the work. By going through one module to the other we create the model through which ABAQUS CAE generates a file (input) which can be submitted to the ABAQUS implicit or explicit in order to perform the analysis. After the completion of the analysis the implicit or explicit unit propagates the required result or information to ABAQUS CAE in-order to help us in monitoring growth or progress of the job after submitting it and then generates the required output database. After the analysis of model, deformation of the structure and high stressed region is seen in the visualisation module.

The ABAQUS model contains the following information:

- The geometry in discretized form
- Properties defined to element section
- Various material data
- Loads and Boundary condition requiring
- Type of analysis
- Output request

3.2. Finite element model

In the present work, ABAQUS CAE is used to model the FRP-concrete hybrid beams and the shear strength of the concrete-FRP interaction is investigated. Firstly, discrete parts of the hybrid beam was modelled such as I-section, concrete layer, shear connectors, bearing plate and reinforcement bars. Further material properties were assigned to each part and assemble together in the assemble module. After assigning the mesh, structure was analysed in monotonic concentrated loading. The detailed description of each module is given in the following sections.

3.2.1 Part module

In this simulation, 3D deformable solid parts are used to generate the concrete layer, web and flanges FRP I-beam. Stiffeners of L & T shaped were also made by 3D deformable solid, while the bearing plates were made up of non-deformable discrete rigid. The reason behind this is that the bearing plates adopted in the experiments were of steel and the flexural rigidity of plates was much larger than that of FRP beam. A reference point is also provided on the bearing plate for providing loads and boundary conditions as shown below in figure 3.1. Bearing plate is converted from solid to shell in order to provide interaction with the concrete slab. Deformable solid parts were used to generate steel re-bars and connectors.

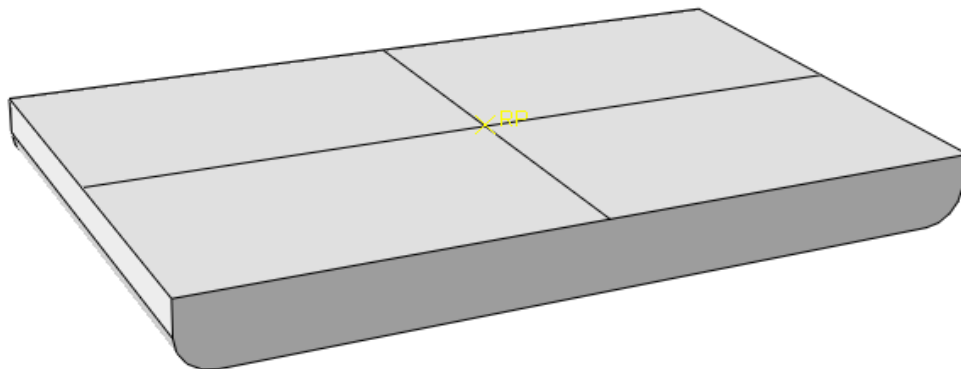


Figure 3.1 Bearing plate

Dimensions of various parts involved in this analysis are given in Table 3.1.

Table 3.1 Specifications of various parts

Parts	Thickness (mm)	Length (mm)	Width (mm)	Depth (mm)	Diameter (mm)
I-section	6.5	1200	75	150	-
Concrete	100	1200	75	100	-
Bearing plate	6.5	75	50	6.5	-
L-Stiffener	6.5	34.25	34.25	122	-
T-stiffener	6.5	34.25	68.5	122	-
Steel bars	-	-	-	-	8
Stirrups	-	-	-	-	6
Shear connector	-	106.5	-	-	8
Studs	-	56.5	-	-	20
Cap	-	4	-	-	25

3.2.2 Material property

In the FE model, non-linear material properties were provided to FRP I-section, bearing stiffeners and shear connectors. The brief explanation is given next.

(i) Concrete layer

Material non-linearity in reinforced cement concrete slab is provided by adopting concrete damaged plasticity (CDP) model. Parameters of CDP analysis depends on the uni-axial compressive and tensile stress-strain curve and based on the flow plasticity theory. This theory helps in analyzing the plastic behavior by assuming a flow rule, which helps to describe the extent to which the material has been deformed. When concrete is subjected to severe state of inelastic stress, a significant change volume occurs which is known as dilation.

A typical compressive stress-strain curve for concrete is shown in Figure . Initially for the linear elastic range, stress is proportional to strain and the value of limit stress is taken as $0.4f_{cm}$ and for the parabolic portion, i.e., non-linear the stress ranges from $0.4f_{cm}$ to f_{cm} , where f_{cm} is the ultimate strength. The slope of the stress-strain curve, i.e., $\tan\alpha$ represents the young modulus of concrete. The stress in non-linear region (σ_c), i.e., $0 < \varepsilon_c < \varepsilon_{cu1}$ can be determined by using Eq. (3.1)

$$\frac{\sigma_c}{f_{cm}} \approx \frac{\eta k - \eta^2}{1 + (k - 2)\eta} \quad (3.1)$$

$$\eta = \frac{\varepsilon_c}{\varepsilon_{c1}}, \quad \varepsilon_{c1} = 0.7 f_{cm}^{0.31} \leq 2.8, \quad k = 1.05(E_c \times |\varepsilon_{c1}|) / f_{cm} \quad (3.2)$$

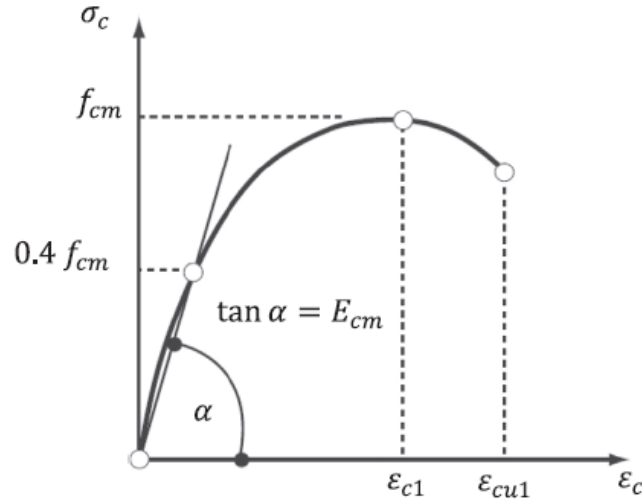


Figure 3.2 Compressive stress-strain curve of concrete.

In case, concrete having characteristic compressive strength ranging from 12 to 50 MPa, the nominal ultimate strain is assumed to be 0.0035. After the peak stress, softening occurs and the stress in this region is calculated by Eq. (3.3)

$$\sigma_c = \left(\frac{2 + \gamma_c f_{cm} \varepsilon_c}{2 f_{cm}} + \gamma_c \varepsilon + \frac{\gamma_c}{2 \varepsilon_c} \varepsilon^2 \right)^{-1} \quad (3.3)$$

Where γ_c is taken as 1.7. Failure of the concrete under tension and compression is calculated by damage variable d_c and d_t , respectively. The expression for damage variable in compression is given by the Eq. (3.4)

$$d_c = 1 - \frac{\sigma_t E_c^{-1}}{\varepsilon_t^{pl} \left(\frac{1}{b_t} - 1 \right) + \sigma_t E_c^{-1}} \quad (3.4)$$

When these two variables of damage are equal to zero there is no damage in concrete otherwise when the variables value are equal to one it represents that the concrete has been fully damaged. The damage variable in case of compression is related to plastic strain (ε_c^{pl}) which varies proportional to strain in inelastic zone (ε_c^{in}), i.e.,

$$\varepsilon_c^{in} = \varepsilon_c - \sigma_t E_c^{-1} \quad (3.5)$$

The plastic strain can be calculated by

$$\varepsilon_c^{pl} = b_c \varepsilon_c^{in} \quad (3.6)$$

The above equation has been determined by using a factor b_c which is constant and ranging from $0 < b_c < 1$.

In the tension zone, the stress varies proportionally to strain until there is no emergence of cracks in concrete and after the crack starts to propagate the stress reduces non-linearly to zero value.

When d_t is greater than zero and the maximum principle strain in plastic is positive crack propagation in concrete starts. At the point of propagation of damage the crack direction and the maximum principle strain in plastic region direction are orthogonal. As per the ABAQUS manual, at zero stress the value of strain is taken as ten times the strain at the point of failure. The damage variable in tension d_t depends on ε_t^{pl} . The value for constants b_c and b_t are assumed to be 0.7. The expression for damage is given below in the Eq. (3.7)

$$d_t = 1 - \frac{\sigma_t E_c^{-1}}{\varepsilon_t^{pl} \left(\frac{1}{b_t} - 1 \right) + \sigma_t E_c^{-1}} \quad (3.7)$$

$$\varepsilon_t^{pl} = b_t \varepsilon_t^{in} \quad (3.8)$$

Table 3.2 Elastic properties for concrete.

Young modulus (N/mm ²)	Poisson's ratio
25000	0.18
150000000	0.45

Table 3.3 Concrete plasticity damage properties

Dilation angle	Eccentricity	Fb ₀ /fc ₀	K	Viscosity parameter
13	0.1	1.16	0.7	0

Table 3.4 Compressive behavior properties for concrete.

Yield stress (N/mm ²)	Inelastic strain
16.75	0
20.00	0.0020
25.00	0.0035

Table 3.5 Tensile behaviour properties for concrete.

Yield stress (N/mm ²)	Inelastic strain
3	0
4	0.012
5	0.020

(ii) Bearing plate

In order to avoid the deformation of bearing plate, the bearing plate was made with discrete rigid part. Due to its rigid nature no property was assigned. Stress concentration under the bearing plate was reduced by providing the high fillet radius of 0.006 at the edges.

(iii) FRP I-section and stiffeners

Due to orthotropic nature of the laminates, composite lay-up technique has been selected to provide the material properties to I-sections and stiffeners. Equivalent material properties of FRP I-section and stiffeners are presented in Table 3.6. Hashin damage failure criteria is considered to investigate the failure of the laminate in tension and/or compression under the flexural loading. Hashin failure criteria for matrix and fiber damage is given as follows:

Matrix tension failure ($\sigma_{22} + \sigma_{33} > 0$):

$$(\sigma_{22} + \sigma_{33})^2 / Y_t^2 + (\sigma_{23}^2 - \sigma_{22}\sigma_{33}) / S_{23}^2 + (\sigma_{12}^2 - \sigma_{12}^2) / S_{12}^2 = 1 \quad (3.9)$$

Fibre tension failure ($\sigma_{11} < 0$):

$$\sigma_{11}^2 / X_t^2 + (\sigma_{12}^2 + \sigma_{13}^2) / S_{12}^2 = 1 \quad (3.10)$$

Matrix compression failure ($\sigma_{22} + \sigma_{33} < 0$):

$$(\sigma_{22} + \sigma_{33}) / Y_c \times [(Y_c / 2S_{23})^2 - 1] + (\sigma_{22} + \sigma_{33})^2 / 4S_{23}^2 + (\sigma_{12} + \sigma_{13})^2 / S_{12}^2 = 1 \quad (3.11)$$

Fibre compression failure ($\sigma_{11} < 0$):

$$\sigma_{11} = -X_c \quad (3.12)$$

Fibre-Matrix shear failure ($\sigma_{11} < 0$):

$$\sigma_{11}^2 / X_c^2 + \sigma_{12}^2 / S_{12}^2 + \sigma_{13}^2 / S_{13}^2 = 1 \quad (3.13)$$

Table 3.6 Elastic properties (MPa) of FRP I-section.

E_1	E_2	E_3	ν_{12}	ν_{13}	ν_{23}	G_{12}	G_{13}	G_{23}
27950	8000	4000	0.28	0.28	0.21	2380	2380	1170

Table 3.7 Different strengths (N/mm²) of flange and web elements of FRP I-section.

Longitudinal tensile strength	Longitudinal compressive strength	Transverse tensile strength	Transverse compressive strength	Longitudinal shear strength	Transverse tensile strength
400000	330000	73000	55000	60000	17000

Damage evolution is used to reduce the stiffness of the laminate (flange and web), after the failure of the layers of laminate. Damage evolution helps in explaining the behaviour of the material after the post damage initiation, i.e., it explains the rate of degradation of the stiffness of the material after the criteria for damage initiation is satisfied. Stress in the layers after degradation is calculated by

$$\sigma = (1 - D)\sigma_d \tag{3.14}$$

Where, σ_d is the stress generated due to undamaged response. Here, D is the overall damage variable, which captures the effect of all the combined active damage mechanism. The fracture occurs when $D = 1$, i.e., point of material has fully failed.

For an elastic-plastic material, the manifestation of damage occurs in two parts

- (i) Softening of the yield stress
- (ii) Degradation of the elasticity

The law of damage evolution can be explained either in the form of fracture energy or equivalent plastic displacement. In both approaches, characteristic length of element is taken into account. In damage evolution, viscosity coefficient for compressive and tensile direction in longitudinal and transverse case is taken as 0.0004, while the fracture energy of the laminates is shown in Table 3.8.

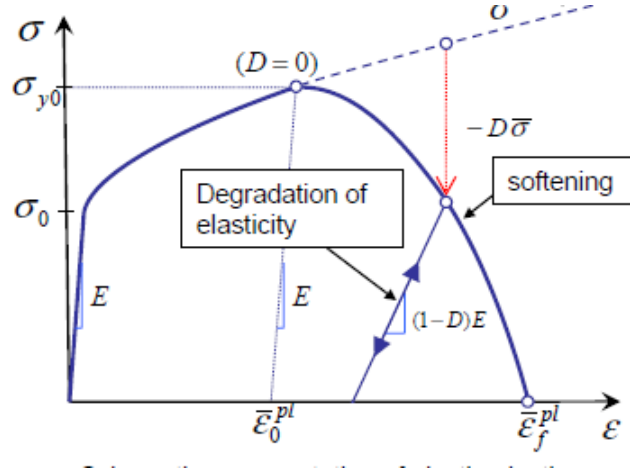
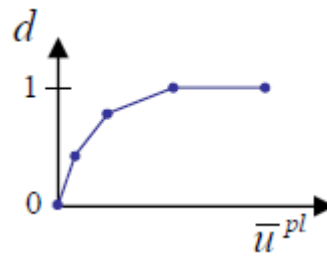
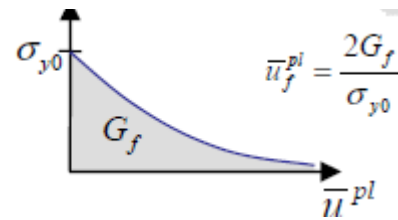


Figure 3.3 Elastic-plastic material with progressive damage



Displacement based damage evolution



Energy based damage evolution

Figure 3.4 Damage evolution criteria.

Table 3.8 Damage evolution properties (fracture energy, N-mm) of FRP I-section.

Longitudinal tensile	Longitudinal compressive	Transverse tensile	Transverse compressive
91.6	79.9	0.22	1.1

(iv) Shear connector and steel bars

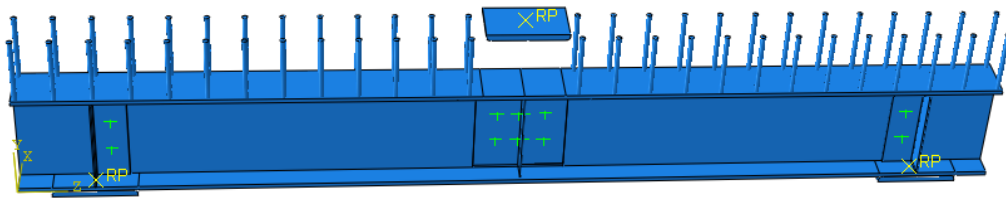
Elastic and plastic properties of mild steel are provided to the shear connectors and reinforcement bars of slab. Non-linear tensile stress strain data (Table 3.9) is used to model the non-linear behavior of connectors and bars.

Table 3.9 Plastic properties for steel bars.

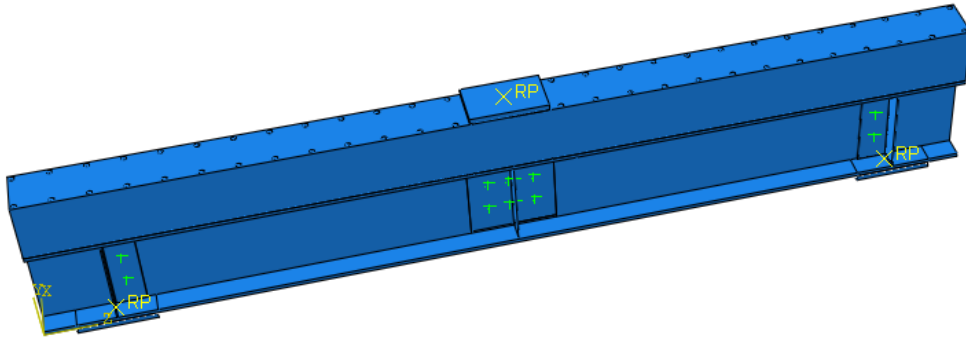
Yield stress (N/mm ²)	Plastic strain
550	0
750	0.02
850	0.04

3.2.3 Assembly

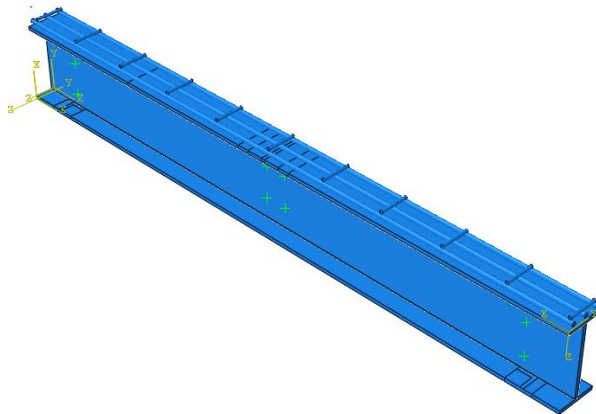
In this module, all discrete parts are assembled together to perform the three-point bending test. For assembling, first step is to create the various instances of independent nature of meshing and after that translate the various instances (parts) as per the required assembly. After placing the one rebar and shear connector, ‘linear pattern’ tool is used to copy and place the required numbers of rebars and connectors as per the desired spacing. Assembled parts of concrete-FRP hybrid I-beams is shown in Figure 3.5



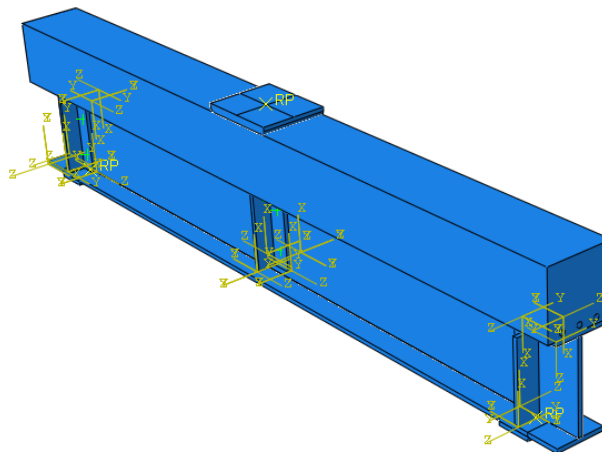
(a) Beam with shear connectors



(b) Beam with shear connectors and reinforced concrete slab



(c) Beam with steel reinforcement



(d) Beam with adhesive connection of concrete layer and FRP I-beam.

Figure 3.5 Hybrid concrete-FRP I-beam with shear connectors and reinforcement.

3.2.4 Interaction

In the experimental investigation, it was observed that hybrid concrete-FRP I-beam fails due to the failure of shear connectors and/or web-flange junction failure of I-beam. Therefore, interaction of different parts plays the vital role in the prediction of the flexural strength of hybrid FRP-concrete I-sections. Different interaction technique provided in the simulation is explained in the following sections:

(i) General contact

General contact helps in providing interaction which allows you to make contact between many regions through a single interaction. Using this technique, interactions are provided between the bearing plates with concrete, and bottom flange surface with bottom bearing plate.

(ii) Tie interaction

Tie interaction is provided in case of L- and T-shaped bearing stiffener with the flange of I-section. It is required to resist the penetration of the stiffeners in to the flange. In this interaction, bottom edge of stiffener is master surface and the surface of the laminate below the bearing stiffener is considered as slave surface.

(ii) Embedded interaction

This type of interaction is used to provide the surface interaction of reinforcement bars and shear connectors with concrete. In this technique, embedded region considered as bars and connectors, while the host region is considered as concrete FRP.

(iii) Surface to surface contact

These types of interactions are generally used for providing cohesive interaction, i.e., contact nonlinearity. At the web-flange junctions of FRP I-beam cohesive interaction is provided, it is because web-flange junctions of FRP I-beams are very prone to failure under the flexural loading. Surface of the flange is considered as master surface while the surface of web (thickness x length) is considered as slave surface. In the contact properties, normal behavior is chosen and cohesive behavior and damage is chosen. Cohesive properties are presented in Tables 3.10-3.12

Table 3.10 Stiffness properties for FRP in N/mm.

K_{nn}	K_{ss}	K_{tt}
1700	800	800

Table 3.11 Damage initiation properties (N/mm²)

Normal only	Shear mode-I	Shear mode-II
30	25	25

In this energy is chosen as the mode mix ratio with linear softening having Benzeggagh-Kennane as the specific mixed mode behavior. The value for power law/BK components is taken equal to 1.45.

Table 3.12 Evolution properties (N-mm) for cohesive layer.

Normal fracture energy	Shear mode-I fracture shear energy	Shear mode-II fracture energy
0.09	0.9	0.9

(v) Fasteners

This is generally used to join the two or more surfaces. In the present case, they are used for joining L & T-shaped bearing stiffeners to the web of I-section. For this, firstly attachment point are created at particular offset from the edges of the stiffener. Further the fastener of radius 10 mm was provided at the attachment points as shown in Figure 3.6

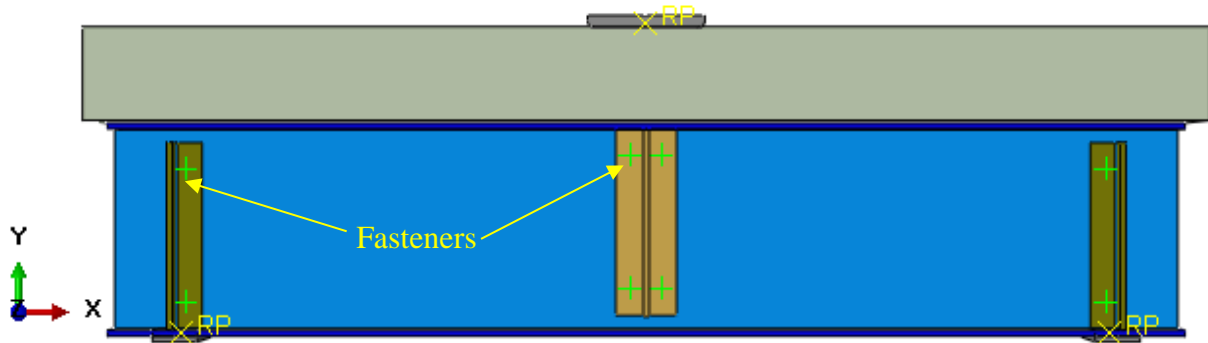


Figure 3.6 Connection of stiffeners using fasteners.

3.2.5. Loading step

For the analysis, static general procedure with time period of 2 second is considered. Flexural behavior is studied under the displacement control mode. In which size of initial increment is 0.0001, whereas minimum and maximum size of increment are 1×10^{-12} and 2, respectively.

3.2.6. Boundary conditions

Simply supported boundary conditions were applied at the ends of the beams as shown in the Figure Along with, torsional boundary conditions were applied at the end of the compression

flange (Figure). As stated earlier, this study is performed under the displacement control mode. Therefore displacement of 50 mm is provided at the reference point of the bearing plate. Bearing plate is restrained to deflect in perpendicular to the direction of load applied and as well as torsion is also restrained as shown in Figure 3.7

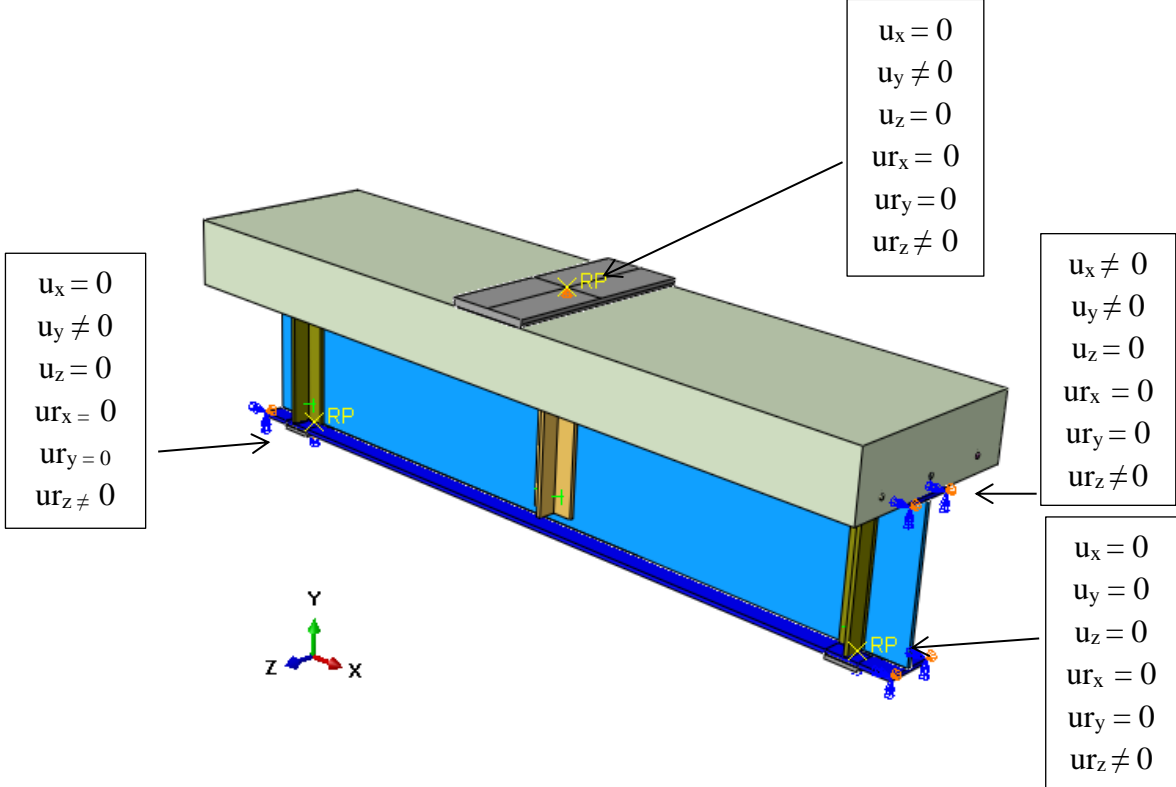


Figure 3.7 Description of boundary conditions.

3.2.7. Meshing

Meshing or discretization is generally carry out in FE analysis as it reduces the degree of freedom from infinite to finite and thus provide ease in solution. Meshing thus helps in breaking the domain into pieces where each piece represents an element which helps in applying the FE technique. In this study, combination of solid elements and shell elements were adopted from the ABAQUS library and utilized for modeling the three-point bend test specimen. Continuum 3-D eight node reduced integration elements C3D8R were used to model the concrete slab and the reinforcing steel re-bars. In order to avoid the numerical imprecisions, the element shapes satisfies the aspect ratio and shape for solid and shell elements as explained in ABAQUS. The meshes are having a uniform size. The bearing plates are modeled using 3 dimensional 4 node rigid element R3D4, i.e., four node element type. The stiffening elements (L & T) shapes were also modeled by C3D8R. In order to refine the mesh variable densities were provided to the various elements.

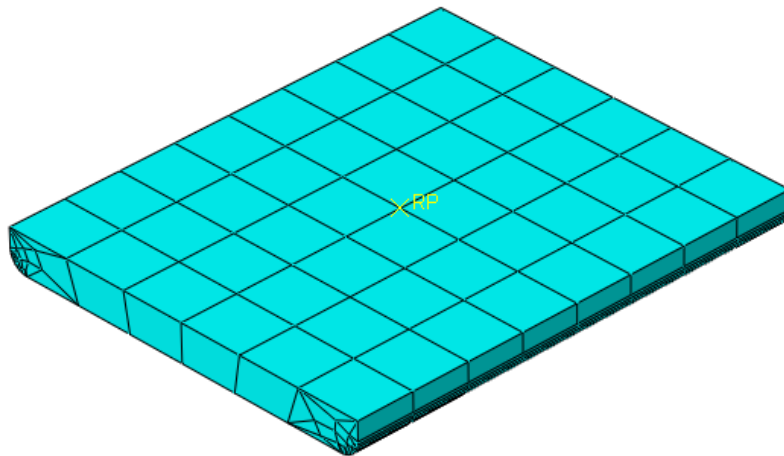


Figure 3.8 Discrete rigid bearing plate

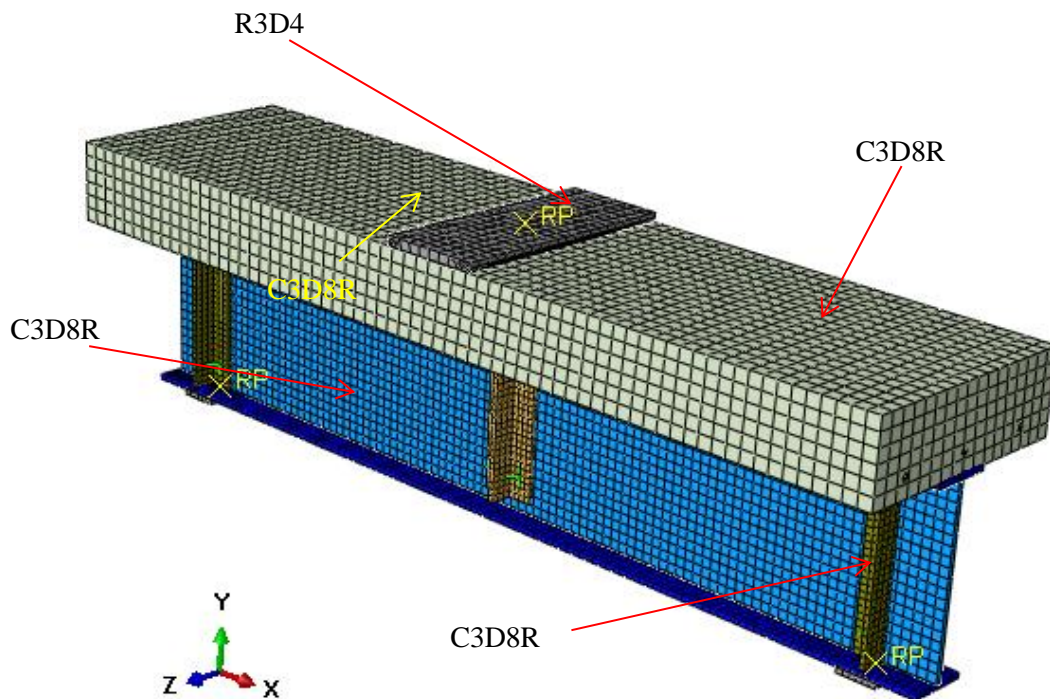


Figure 3.9 Meshing of various parts of the model and different element type used

Chapter 4 Flexural Study of Hybrid Beams

4.1 Verification of the FE model

This section presents the comparison of the flexural responses of the hybrid beams obtained from the proposed numerical model (135) and published experimental study (Nguyen et al. 2015). Hybrid beam modeled in ABAQUS have fiber reinforced concrete layer over the compression flange of FRP I-section. Shear connectors are used to connect the concrete layer with flange of FRP I-section as shown in the Figure 4.1. Flexural response obtained from the numerical model is shown in the Figure 4.2 (Nguyen et al. 2015). It is observed that the proposed modeling technique shows the good agreement of numerical and experimental results. Compression failure of the concrete layer was noticed under the bearing plate. The red region under the bearing plate in the Figure 4.3 shows the high stress concentration. Previous studies [Singh and Chawla (2019), Chawla and Singh (2019), Yin and Bank (1999)] have shown that web-flange junction of the FRP I-section is the weaker portion of the beams and the first mode of failure of beams is the failure of web-flange junction. But the addition of the concrete layer over the compression flange of the FRP I-section enhances the flexural strength, and the failure mode of the beams is compression failure of concrete layer.

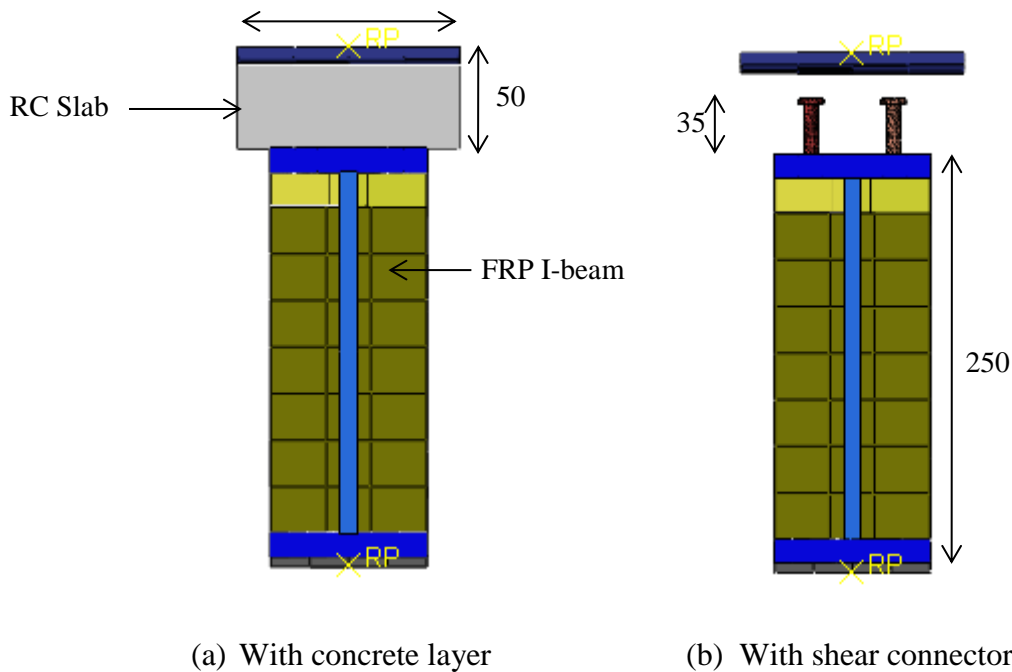


Figure 4.1 Concrete-FRP hybrid beam modelled in ABAQUS. (All dimensions are in mm)

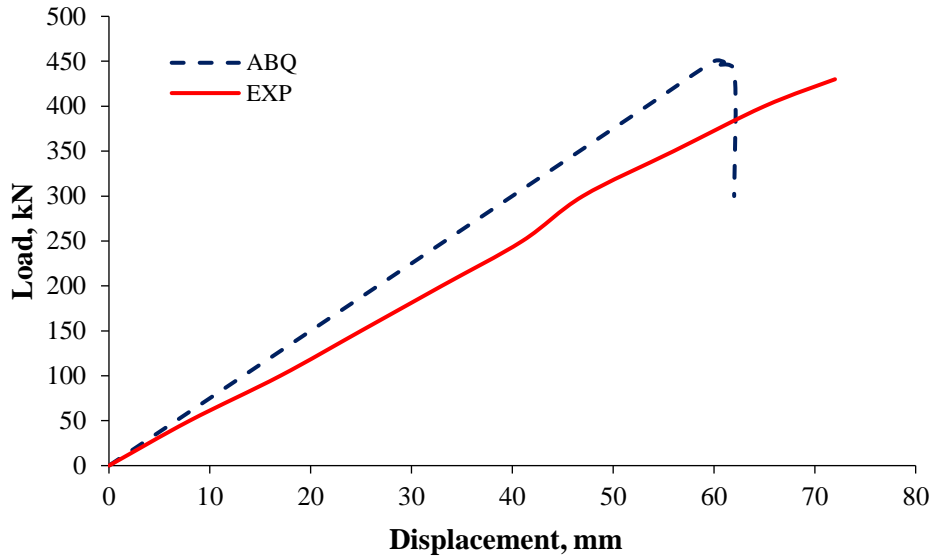


Figure 4.2 Comparison of load-deflection response of the hybrid beam obtained in ABAQUS with published results (Nguyen et al.2015).

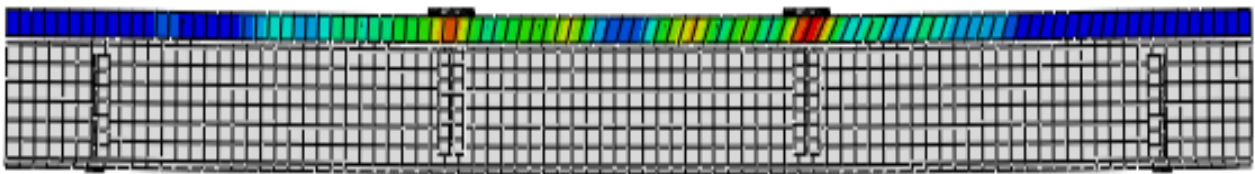


Figure 4.3 Stress variation in the concrete layer under three-point bending of hybrid beams.

4.2 Parametric study

After the verification of the numerical results with published results, a parametric study is performed on the beams having different geometric configuration and different degree and type of connections of RC slab and I-beam. Flexural study is conducted on the beams having different spacing and sizes of bolts. Furthermore, parametric study is performed on FRP beams having different length-to-depth (L/d) ratios, web depth-to-thickness (D/t) ratios and different width of reinforced concrete slab (b_c). In this analysis, influence of the different geometric properties of RC slab and I-section on the failure and service loads is evaluated. Service and failure loads is determined for beams having L/d ratios 3, 5 and 7; width of flange of I section-to-thickness ratios 11, 15 and 19. The ratio of depth of web-to-thickness of I-section is considered as 27, 31 and 35. All the above parametric values are analyzed with the different width of RC slab, i.e., 150, 300 and 450 mm. In the RC slab, steel bars of 10 mm diameter have center-to-center spacing of 100 mm, therefore 2, 3 and 5 longitudinal bars are provided in the slab of width 150 mm, 300 mm and 450 mm, respectively. Service load is calculated from the load-deflection response of the beam and it is the load corresponding to serviceable deflection ($L/300$). On the other hand, failure load

is minimum of first ply failure load of the laminate and crushing load of the RC slab. The parametric study performed on the FRP-concrete hybrid beams is explained in the following sections:

4.2.1 Size and spacing of shear connectors

This section presents the flexural response of the beams having different length and spacing of shear connectors. Figure 4.4 shows the flexural deformation of the hybrid beam with shear connectors. It is observed that end of shear connectors deformed due to the bending beam. From Figure 4.5 and 4.6, it is noted that as the horizontal distance decreases and density of shear connectors decreases consequently flexural stiffness of the beam (slope of load-deflection curve) decreases. On the other hand, as the vertical distance of the shear connector from the edge of bearing plate decreases, i.e., length of the shear connectors increases, the strength and stiffness of the hybrid beam increases.

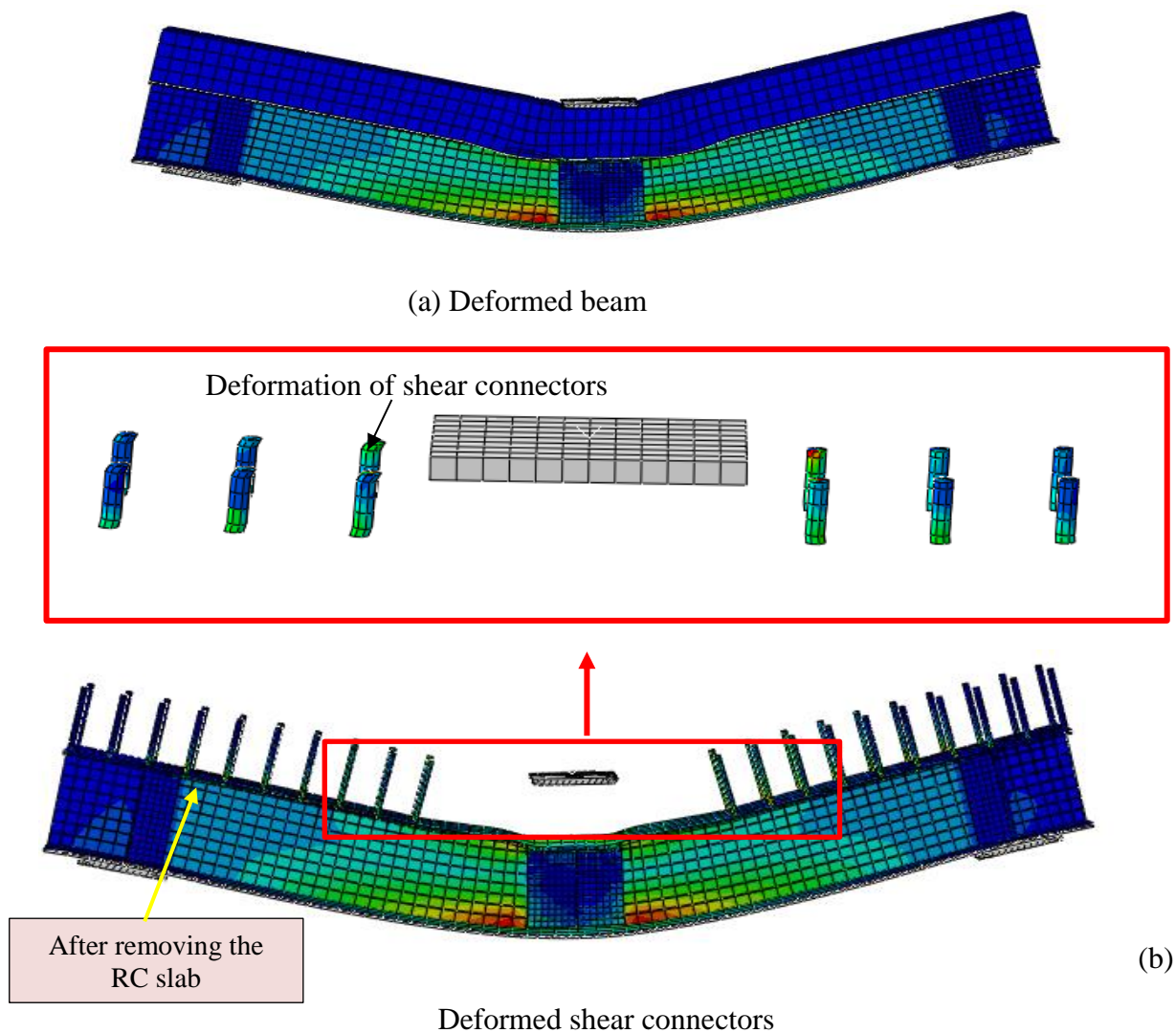


Figure 4.4. Flexural behavior of FRP-concrete hybrid beam.

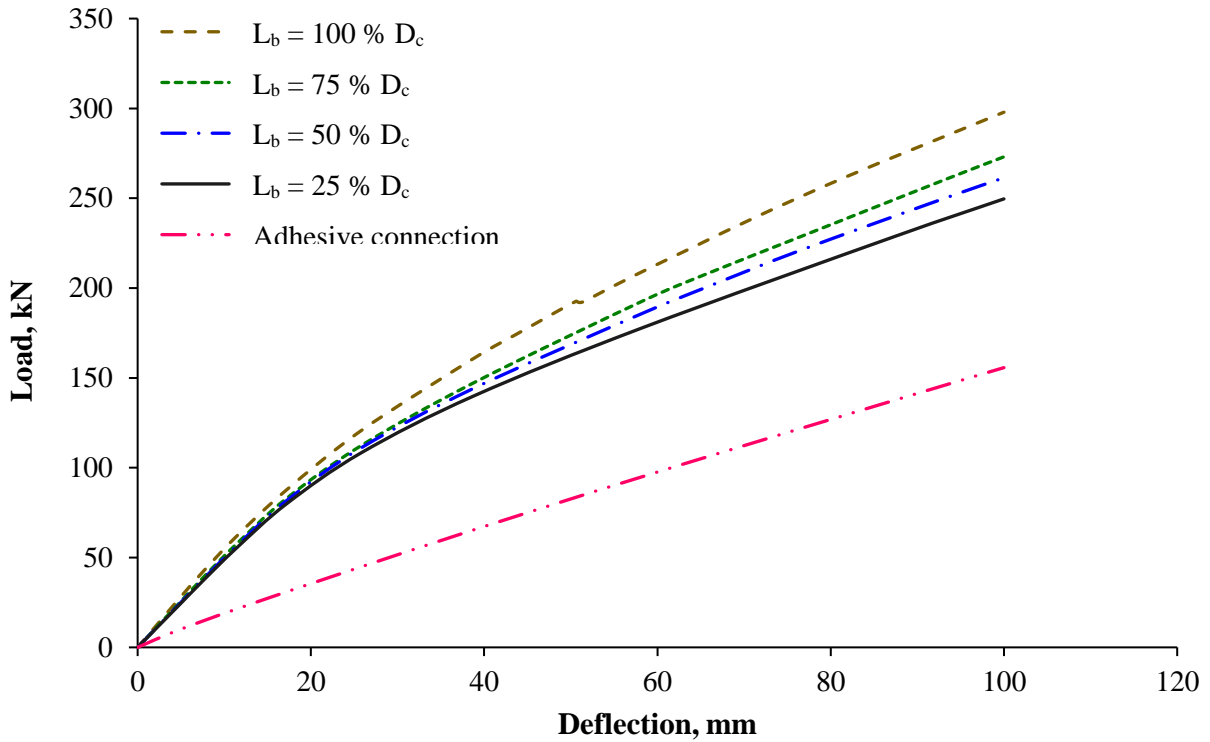


Figure 4.5. Flexural response of the beams with different sizes of shear connectors.

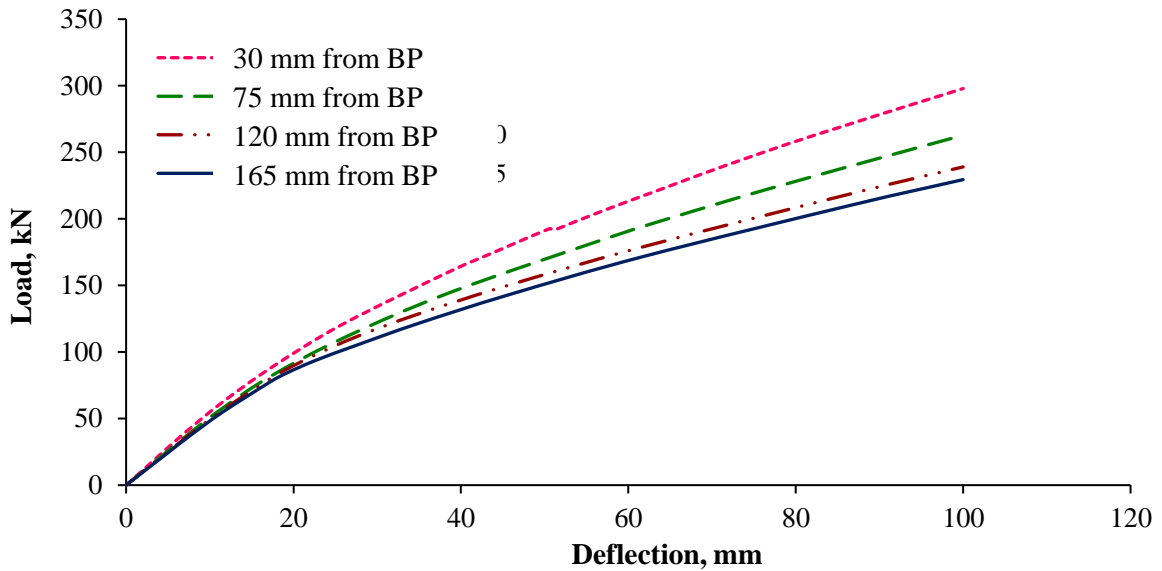


Figure 4.6. Flexural response of the beams with different spacing of shear connectors.

4.2.2 Influence of variation of length-to-depth ratio of I-beam

The FRP beams having low L/d ratio are prone to fail by local buckling. Therefore, failure and service loads are determined for beams having different length such as 600 mm, 900 mm and 1200 mm while the same width and depth of the I-beams, i.e. 75 and 150 mm, respectively. In each beam, supports are provided at the distance of 75 mm from the ends, so that the L/d ratio is

maintained as 3, 5 & 7. Along with the variation of L/d ratios, width-to-thickness (b/t) of concrete layer is also varied. The service and failure load of the beams having different L/d ratio is shown in Figure 4.8. It is observed that with decrease in the length of the beam, flexural stiffness of the beam increases. The failure and service load is lower for the beams having higher L/d ratio as shown in Figure 4.8. The failure mode in each beams was failure of web-flange junction.

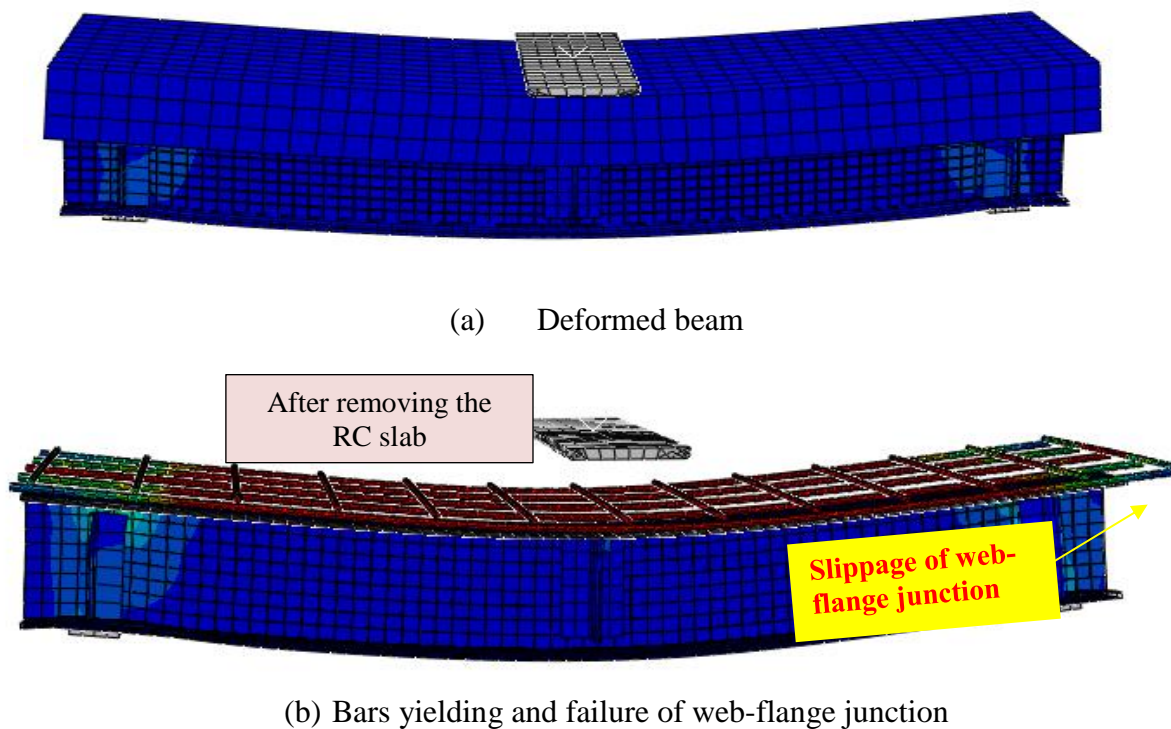


Figure 4.7. Flexural deformation of the beam having L/d ratio 7 with RC slab of width 300 mm.

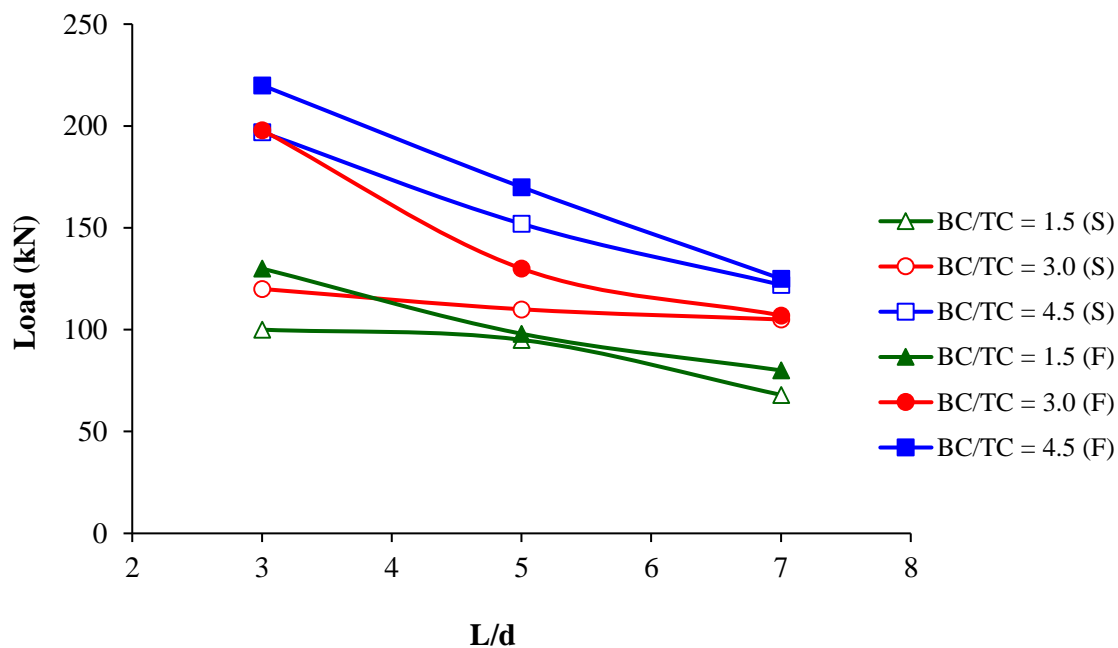


Figure 4.8. Effect of L/d ratio on service and failure loads.

4.2.3 Influence of flange width of I-beam

In another study, flange width (B) of I-beam is varied as 75, 100 and 125 mm, while the thickness (t) in each case is 6.5 mm and the B/t ratio is 11, 15 and 19. In order to investigate the effect of addition of RC slab on the flexural strength of FRP I-beam, the width of RC slab (b_c) is varied as 150, 300 and 450 mm. It is noted that in each beam failure of web-flange junction of FRP I-beam occurred as shown in Figure 4.9. After failure RC slab moves along with the flange element due to shear connectors between the RC slab and top flange. From Figure 4.10, it is observed that some beams same failure and service load, it is due to the pre-mature failure of the web-flange junction of the I-beams. Hence, it is stated that addition of RC slab enhances the flexural stiffness, i.e., service load and also enhance the strength of web-flange junction.

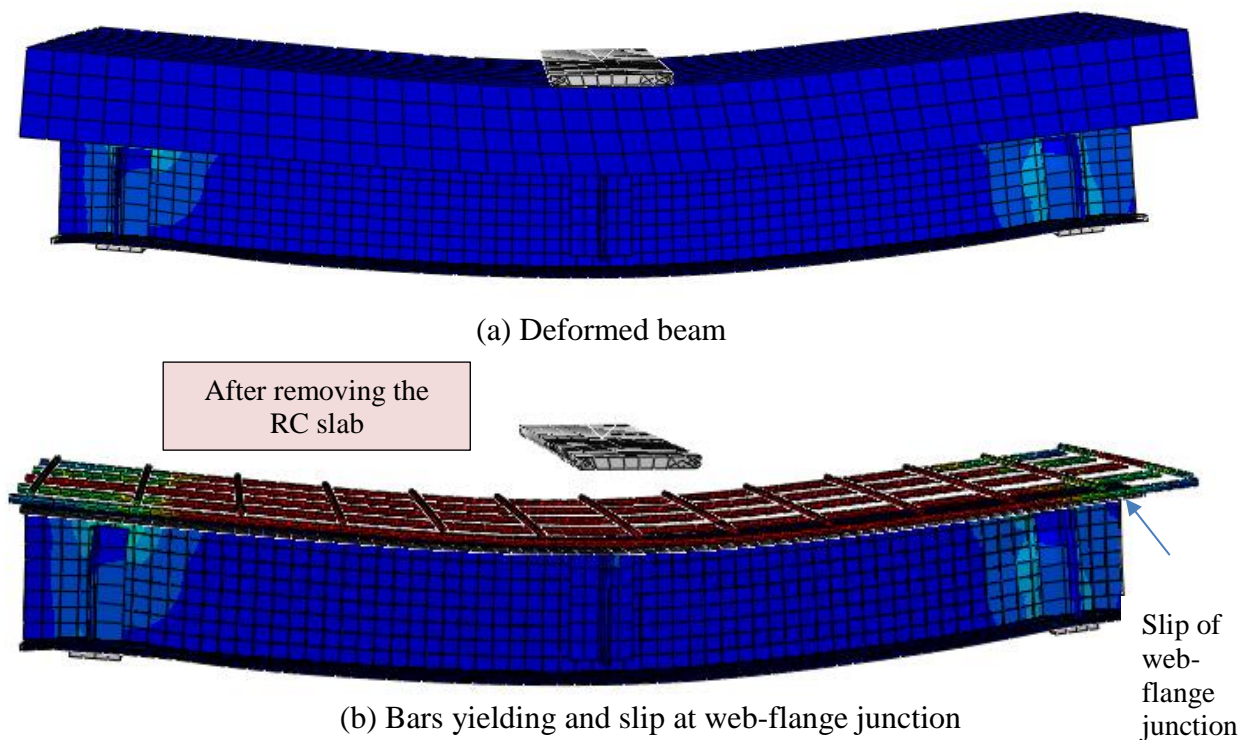


Figure 4.9. Flexural deformation of the beam having B/t ratio 11 with RC slab of width 300(mm).

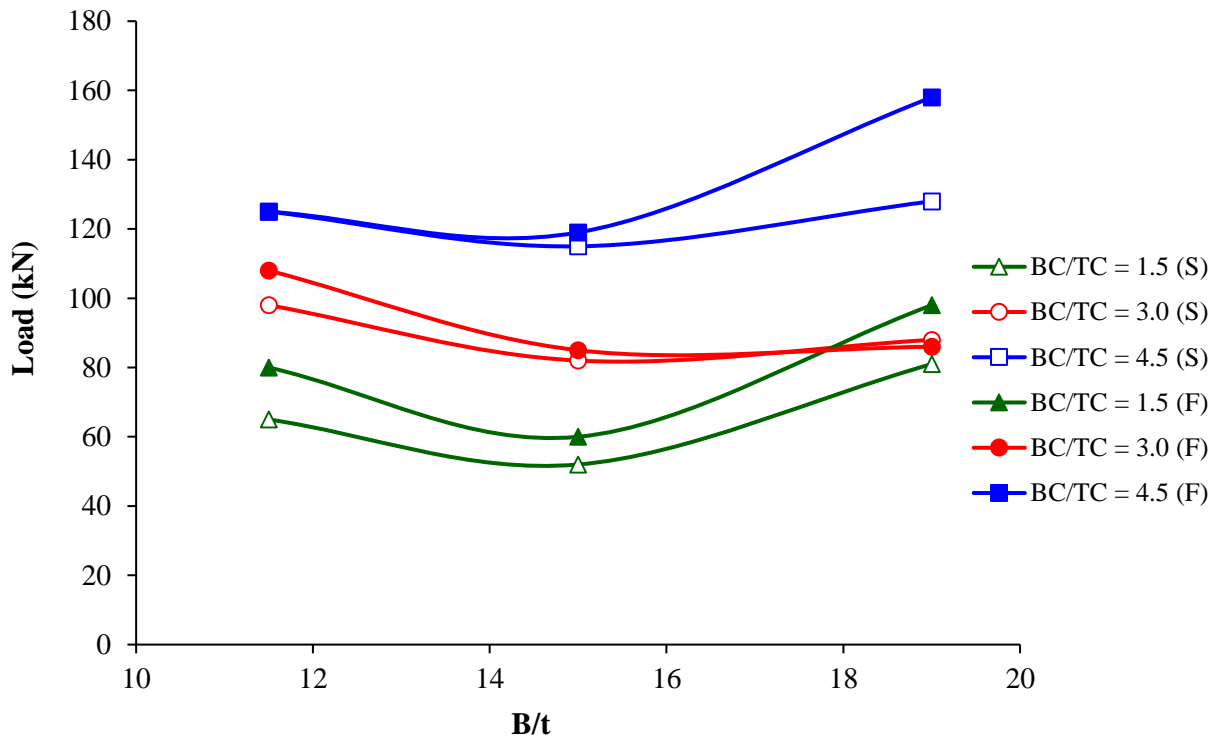


Figure 4.10. Effect of B/t ratio on service and failure load.

4.2.4 Effect of depth I-beam

This section presents the influence of web depth and width of RC slab on the flexural response of the I-sections. The depth of the web is taken as 175, 200 and 225 mm with constant thickness 6.5 mm. Figure 4.11 shows that beams failed by failure of web-flange junction. It is noted that failure and service load increases with increase in the depth of the beams (Figure 4.12). Along with the lateral stability also increases with increase in the width of RC slab. Hence, the local buckling of the web was not observed and the failure of the web-flange junction occurred.

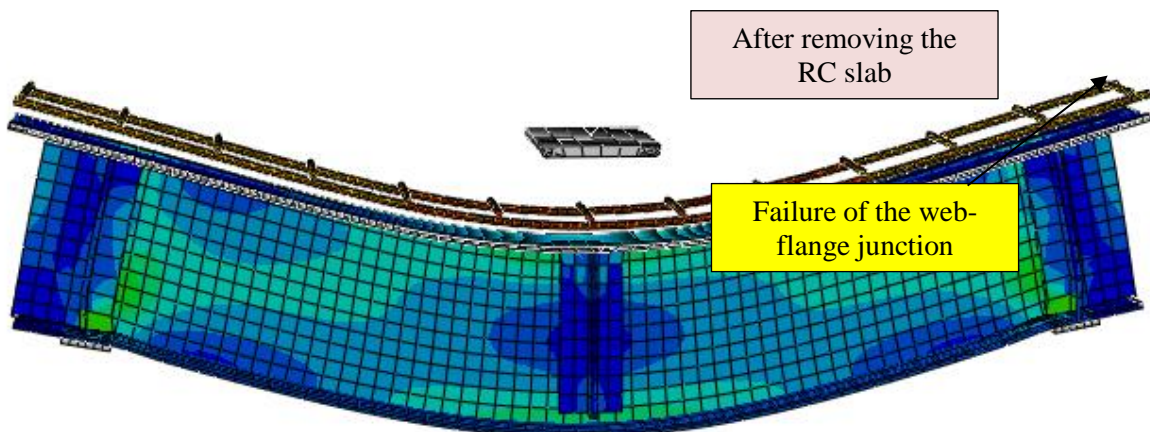


Figure 4.11. Failure of the web-flange junction.

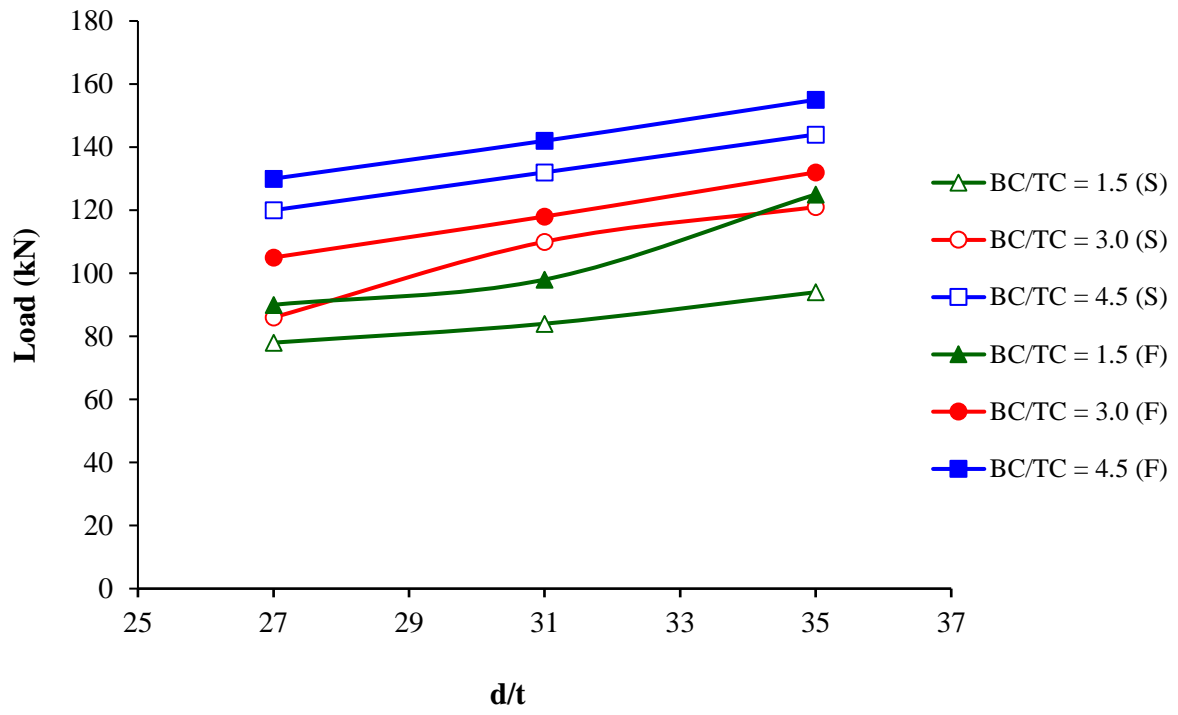


Figure 4.12. Effect of D/t ratio on service and failure loads.

Chapter 5 Conclusions

5.1 Introduction

In this study, flexural behavior of concrete-FRP hybrid beams is determined. Beams are modeled in finite element software ABAQUS. Shear connection between the FRP beams and RC slab is made using shear connectors and adhesive bonding. Web and flange elements of I-beams are connected with cohesive layer, because it is the weaker portion in the FRP I-beams and is highly prone to fail under three-point loading. Accuracy of the numerical model is verified by comparing the results with published experimental study. Further, the parametric study is performed on beams having different size and spacing of shear connectors. Alongwith, failure and service load of hybrid beams is determined for different geometric configuration of I-beams and width of RC slab.

5.2 Conclusions

Based on these results obtained from numerical model, concluding remarks are as follows:

1. The proposed modeling techniques of hybrid FRP-concrete beams using finite element software ABAQUS is effective in producing the same flexural response and failure mode as obtained from experimental testing.
2. Shear connectors helps in improving the strength of concrete-FRP hybrid beams. With increasing the length of shear connectors there is slight improvement in the strength of beam.
3. As density of shear connectors decreases consequently flexural stiffness of the beam (initial slope of load-deflection curve) decreases.
4. The strength and stiffness of the hybrid beam increases with increase in the length of the shear connectors.
5. With decrease in the length of the beam, flexural stiffness of the beam increases. The failure and service load is lower for the beams having higher L/d ratio.
6. From the flexural study of the beams having different B/t ratio, it is observed that some beams same failure and service load, it is due to the pre-mature failure of the web-flange junction of the I-beams. Hence, it is stated that addition of RC slab enhances the flexural stiffness, i.e., service load and also enhance the strength of web-flange junction.
7. Addition of reinforced concrete slab over the FRP I-beams, reduces the chances of local buckling of the flange and web of the I-beam.

REFERENCES

- Alnahhal, W., Aref, A., & Alampalli, S. (2008). Composite behavior of hybrid FRP-concrete bridge decks on steel girders. *Composite Structures*, 84(1), 29-43.
- Araba, A. M., & Ashour, A. F. (2018). Flexural performance of hybrid GFRP-Steel reinforced concrete continuous beams. *Composites Part B: Engineering*, 154, 321-336.
- Attari, N., Amziane, S., & Chemrouk, M. (2012). Flexural strengthening of concrete beams using CFRP, GFRP and hybrid FRP sheets. *Construction and Building Materials*, 37, 746-757.
- Bank, L. C., & Yin, J. (1999). Failure of web-flange junction in post-buckled pultruded I-beams. *Journal of Composites for Construction*, 3(4), 177-184.
- Canning, L., Hollaway, L., & Thorne, A. M. (1999). An investigation of the composite action of an FRP/concrete prismatic beam. *Construction and Building Materials*, 13(8), 417-426.
- Cao, Q., Zhou, J., Gao, R., & Ma, Z. J. (2017). Flexural behavior of expansive concrete beams reinforced with hybrid CFRP enclosure and steel rebars. *Construction and Building Materials*, 150, 501-510.
- Chakraborty, A., Khennane, A., Kayali, O., & Morozov, E. (2011). Performance of outside filament-wound hybrid FRP-concrete beams. *Composites Part B: Engineering*, 42(4), 907-915.
- Chawla, H., & Singh, S. B. (2019). Stability and failure characterization of fiber reinforced pultruded beams with different stiffening elements, part 2: Analytical and numerical studies. *Thin-Walled Structures*, 141, 606-626.
- Chellapandian, M., & Prakash, S. S. (2019). Behavior of FRP-strengthened reinforced concrete under pure bending-experimental and numerical studies. In *Recent Advances in Structural Engineering, Volume 2* (pp. 663-673).
- Cho, K., Park, S. Y., Kim, S. T., Cho, J. R., & Kim, B. S. (2010). Shear connection system and performance evaluation of FRP-concrete composite deck. *KSCE Journal of Civil Engineering*, 14(6), 855-865.
- Correia, J. R., Branco, F. A., & Ferreira, J. (2009). GFRP-concrete hybrid cross-sections for floors of buildings. *Engineering Structures*, 31(6), 1331-1343.

- Correia, J. R., Branco, F. A., & Ferreira, J. G. (2007). Flexural behaviour of GFRP–concrete hybrid beams with interconnection slip. *Composite Structures*, 77(1), 66-78.
- Correia, J. R., Branco, F. A., & Ferreira, J. G. (2009). Flexural behaviour of multi-span GFRP-concrete hybrid beams. *Engineering Structures*, 31(7), 1369-1381.
- Dagher, H. J., Bannon, D. J., Davids, W. G., Lopez-Anido, R. A., Nagy, E., & Goslin, K. (2012). Bending behaviour of concrete-filled tubular FRP arches for bridge structures. *Construction and Building Materials*, 37, 432-439.
- De Wall, L., Fernando, D., Cork, R., & Foote, J. (2017). FRP strengthening behaviour of concrete bridge deck units. *Engineering Structures*, 143, 346-357.
- Deskovic, N., Meier, U., & Triantafillou, T. C. (1995). Innovative design of FRP combined with concrete: long-term behavior. *Journal of Structural Engineering*, 121(7), 1079-1089.
- Duic, J., Kenno, S., & Das, S. (2018). Performance of concrete beams reinforced with basalt fibre composite rebar. *Construction and Building Materials*, 176, 470-481.
- Fam, A. Z., & Rizkalla, S. H. (2002). Flexural behavior of concrete-filled fiber-reinforced polymer circular tubes. *Journal of Composites for Construction*, 6(2), 123-132.
- Fang, H., Xu, X., Liu, W., Qi, Y., Bai, Y., Zhang, B., & Hui, D. (2016). Flexural behavior of composite concrete slabs reinforced by FRP grid facesheets. *Composites Part B: Engineering*, 92, 46-62.
- Ge, W., Zhang, J., Cao, D., & Tu, Y. (2015). Flexural behaviors of hybrid concrete beams reinforced with BFRP bars and steel bars. *Construction and Building Materials*, 87, 28-37.
- Gonilha, J. A., Barros, J., Correia, J. R., Sena-Cruz, J., Branco, F. A., Ramos, L. F & Santos, T. (2014). Static, dynamic and creep behaviour of a full-scale GFRP-SFRSCC hybrid footbridge. *Composite Structures*, 118, 496-509.
- Gonilha, J. A., Correia, J. R., Branco, F. A., Caetano, E., & Cunha, Á. (2013). Modal identification of a GFRP-concrete hybrid footbridge prototype: Experimental tests and analytical and numerical simulations. *Composite Structures*, 106, 724-733.
- Hall, J. E., & Mottram, J. T. (1998). Combined FRP reinforcement and permanent formwork for concrete members. *Journal of Composites for Construction*, 2(2), 78-86.

- Joo, H. J., Lee, S. S., Yoon, S. J., Park, J. K., & Youn, S. G. (2006). Experimental investigation on the structural behavior of shear connectors used in the FRP and concrete bridge deck system. In *Key Engineering Materials* (Vol. 306, pp. 1355-1360). *Trans Tech Publications*.
- Ju, M., Park, Y., & Park, C. (2017). Cracking control comparison in the specifications of serviceability in cracking for FRP reinforced concrete beams. *Composite Structures*, *182*, 674-684.
- Kim, H. S., & Shin, Y. S. (2011). Flexural behavior of reinforced concrete (RC) beams retrofitted with hybrid fiber reinforced polymers (FRPs) under sustaining loads. *Composite Structures*, *93*(2), 802-811.
- Koaiik, A., Bel, S., & Jurkiewicz, B. (2017). Experimental tests and analytical model of concrete-GFRP hybrid beams under flexure. *Composite Structures*, *180*, 192-210..
- Mendes, P. J., Barros, J. A., Sena-Cruz, J. M., & Taheri, M. (2011). Development of a pedestrian bridge with GFRP profiles and fibre reinforced self-compacting concrete deck. *Composite Structures*, *93*(11), 2969-2982.
- Mendes, P. J., Barros, J. A., Sena-Cruz, J., & Teheri, M. (2014). Influence of fatigue and aggressive exposure on GFRP girder to SFRSCC deck all-adhesive connection. *Composite Structures*, *110*, 152-162.
- Mohamed, H. M., & Masmoudi, R. (2010). Flexural strength and behaviour of steel and FRP-reinforced concrete-filled FRP tube beams. *Engineering structures*, *32*(11), 3789-3800.
- Neagoe, C. A., Gil, L., & Pérez, M. A. (2015). Experimental study of GFRP-concrete hybrid beams with low degree of shear connection. *Construction and Building Materials*, *101*, 141-151.
- Nguyen, H., Mutsuyoshi, H., & Zatar, W. (2015). Hybrid FRP-UHPFRC composite girders: Part 1—Experimental and numerical approach. *Composite Structures*, *125*, 631-652.
- Qazi, S., Michel, L., Ferrier, E., & Limam, A. (2015). Strut-and-tie model for a reinforced concrete wall strengthened with carbon fibre-reinforced polymers. *Composite Structures*, *128*, 87-99.
- Qin, R., Zhou, A., & Lau, D. (2017). Effect of reinforcement ratio on the flexural performance of hybrid FRP reinforced concrete beams. *Composites Part B: Engineering*, *108*, 200-209.
- Saiidi, M., Gordaninejad, F., & Wehbe, N. (1994). Behavior of graphite/epoxy concrete composite

beams. *Journal of Structural Engineering*, 120(10), 2958-2976.

Singh, S. B., & Chawla, H. (2019). Stability and failure characterization of fiber reinforced pultruded beams with different stiffening elements, Part I: Experimental investigation. *Thin-Walled Structures*, 141, 593-605.

Xin, H., Mosallam, A., Liu, Y., Wang, C., & Zhang, Y. (2017). Analytical and experimental evaluation of flexural behavior of FRP pultruded composite profiles for bridge deck structural design. *Construction and Building Materials*, 150, 123-149.

Zou, X., Feng, P., & Wang, J. (2016). Perforated FRP ribs for shear connecting of FRP-concrete hybrid beams/decks. *Composite Structures*, 152, 267-276.